Black Sea Mixed Layer Sensitivity to Various Wind and Thermal Forcing Products on Climatological Time Scales*

A. BIROL KARA, HARLEY E. HURLBURT, AND ALAN J. WALLCRAFT

Oceanography Division, Naval Research Laboratory, Stennis Space Center, Mississippi

MARK A. BOURASSA

Center for Ocean–Atmospheric Prediction Studies, Tallahassee, Florida

(Manuscript received 3 December 2004, in final form 8 June 2005)

ABSTRACT

This study describes atmospheric forcing parameters constructed from different global climatologies, applied to the Black Sea, and investigates the sensitivity of Hybrid Coordinate Ocean Model (HYCOM) simulations to these products. Significant discussion is devoted to construction of these parameters before using them in the eddy-resolving (≈3.2-km resolution) HYCOM simulations. The main goal is to answer how the model dynamics can be substantially affected by different atmospheric forcing products in the Black Sea. Eight wind forcing products are used: four obtained from observation-based climatologies, including one based on measurements from the SeaWinds scatterometer on the Quick Scatterometer (QuikSCAT) satellite, and the rest formed from operational model products. Thermal forcing parameters, including solar radiation, are formed from two operational models: the European Centre for Medium-Range Weather Forecasts (ECMWF) and the Fleet Numerical Meteorology and Oceanography Center (FNMOC) Navy Operational Global Atmospheric Prediction System (NOGAPS). Climatologically forced Black Sea HYCOM simulations (without ocean data assimilation) are then performed to assess the accuracy and sensitivity of the model sea surface temperature (SST) and sea surface circulation to these wind and thermal forcing products. Results demonstrate that the model-simulated SST structure is quite sensitive to the wind and thermal forcing products, especially near coastal regions. Despite this sensitivity, several robust features are found in the model SST in comparison to a monthly 9.3-km-resolution satellite-based Pathfinder SST climatology. Annual mean HYCOM SST usually agreed to within $\approx \pm 0.2^\circ$ of the climatology in the interior of the Black Sea for any of the wind and thermal forcing products used. The fine-resolution ($0.25^\circ \times 0.25^\circ$) wind forcing from the scatterometer data along with thermal forcing from NOGAPS gave the best SST simulation with a basin-averaged rms difference value of 1.21°C, especially improving model results near coastal regions. Specifically, atmospherically forced model simulations with no assimilation of any ocean data suggest that the basin-averaged rms SST differences with respect to the Pathfinder SST climatology can vary from 1.21° to 2.15°C depending on the wind and thermal forcing product. The latter rms SST difference value is obtained when using wind forcing from the National Centers for Environmental Prediction (NCEP), a product that has a too-coarse grid resolution of $1.875^\circ \times 1.875^\circ$ for a small ocean basin such as the Black Sea. This paper also highlights the importance of using high-frequency (hybrid) wind forcing as opposed to monthly mean wind forcing in the model simulations. Finally, there are large variations in the annual mean surface circulation simulated using the different wind sets, with general agreement between those forced by the model-based products (vector correlation is usually >0.7). Three of the observation-based climatologies generally yield unrealistic circulation features and currents that are too weak.

* Naval Research Laboratory Contribution Number NRL/JA/7304/04/0002.

Corresponding author address: Birol Kara, Naval Research Laboratory, Code 7320, Bldg. 1009, Stennis Space Center, MS 39529-5004.
E-mail: kara@nrlssc.navy.mil

1. Introduction and motivation

Given the dynamical importance of heat and momentum exchange at the air–sea interface, ocean general circulation model (OGCM) studies necessitate reliable atmospheric forcing fields that can be used for simulations. The use of quality atmospheric forcing fields is especially important for the Black Sea because there are large uncertainities in the existing heat and wind stress climatologies constructed from local observations. Detailed investigations were performed to compare atmospheric forcing parameters obtained from local datasets (Staneva and Stanev 1998; Schrum et al. 2001). The conclusion was that the existing local atmospheric forcing fields need improvements because the local observational datasets are too sparse in time and space to form realistic climatologies for the Black Sea.

Wind stress and heat fluxes for the Black Sea that have been used for ocean model simulations were mainly constructed from local observations (e.g., Sorkina 1974; Altman and Kumish 1986; Simonov and Altman 1991; Trukhchev and Demin 1992), and they all present large uncertainties (e.g., Staneva and Stanev 1998). For example, climatological wind fields were usually computed from many years of ship observations. However, wind speed and direction, air and sea temperatures, and other meteorological parameters near the sea surface are not routinely measured at many coastal locations and in the interior of the Black Sea where the depth of water is $>$1300 m (Fig. 1). This is even true over the wide northwestern continental shelf where the depth is $<$200 m. Thus, traditional in situ observations are sparse and inhomogeneous. This makes it difficult to obtain complete information on temporal and spatial scales.

When the local climatologies mentioned above were used in forcing OGCMs, they resulted in unrealistic model simulations. In particular, the model study by Oguz and Malanotte-Rizzoli (1996), who examined seasonal variability of the Black Sea, used a monthly mean heat flux climatology (Efimov and Timofeev 1990), which was formed from local datasets. That study indicated the need to reanalyze the heat flux climatology because their model simulations produced unrealistic temperature simulations in the mixed layer. Their simulations also suggested that reducing the original fluxes by one-half might be a reasonable estimate for the winter, and a smaller reduction of the heat fluxes should be sufficient for summer, demonstrating shortcomings of the existing local climatologies in predicting upper-ocean parameters, such as sea surface temperature (SST). Similarly, local climatologies of evaporation and precipitation may induce unrealistic temperature distributions and water mass properties in the surface layer when they are used as atmospheric forcing in model simulations (Oguz and Malanotte-Rizzoli 1996).

Discussions presented above clearly indicate that Black Sea modeling studies need high-quality atmospheric forcing. Wind stress and surface heat flux products from operational models have been exploited as surface forcing for OGCMs in the Black Sea because they provide complete information at all modeled temporal and spatial scales. In addition, a fine-resolution ($0.25° \times 0.25°$) wind stress climatology based on spaceborne scatterometer observations of wind speed and direction is introduced over the Black Sea for the first time. Sensitivity studies are then performed by using these atmospheric products to force an OGCM.

The availability of these atmospheric forcing products raises important questions. 1) How do these products compare with each other and with local datasets in the Black Sea? 2) What is the best wind stress or surface heat flux to use in forcing a Black Sea OGCM? 3) Do operational atmospheric model products provide a more accurate representation of the surface stress experienced by the ocean, or is it better to use their 10-m winds with a parameterized drag coefficient to construct wind stresses? Answers to all of these questions are discussed throughout the text. In addition, we investigate whether or not newly constructed atmospheric forcing products differ from climatologies formed from local observations as reported in earlier Black Sea modeling studies.

As expected, both observation-based climatologies and operational model products have their unique biases, and they can differ significantly in some regions of the global ocean (e.g., Rienecker et al. 1996; Trenberth et al. 2001; Metzger 2003). Thus, the use of these products in OGCM simulations may result in various responses in different regions of the global ocean as shown in many OGCM studies (e.g., Schopf and Loughe 1995; Fu and Chao 1997; Samuel et al. 1999; Ezer 1999; Townsend et al. 2000; Metzger 2003; Lee et al. 2005; Hogan and Hurlburt 2005). In this paper, the focus is to investigate the impact of these climatological forcing fields on Black Sea OGCM simulations. Specifically, in the first part of this paper, we extend the studies of (Staneva and Stanev 1998; Schrum et al. 2001), so that a more-detailed and comprehensive picture of the atmospheric forcing in the Black Sea can be given. In the second part of the paper, an eddy-resolving OGCM with $\approx$3.2-km resolution set up for the Black Sea (Kara et al. 2005a) is forced with these atmospheric forcing fields to answer how they affect model performance in predicting SST. Since SST is the best observed oceanic field of the Black Sea mixed

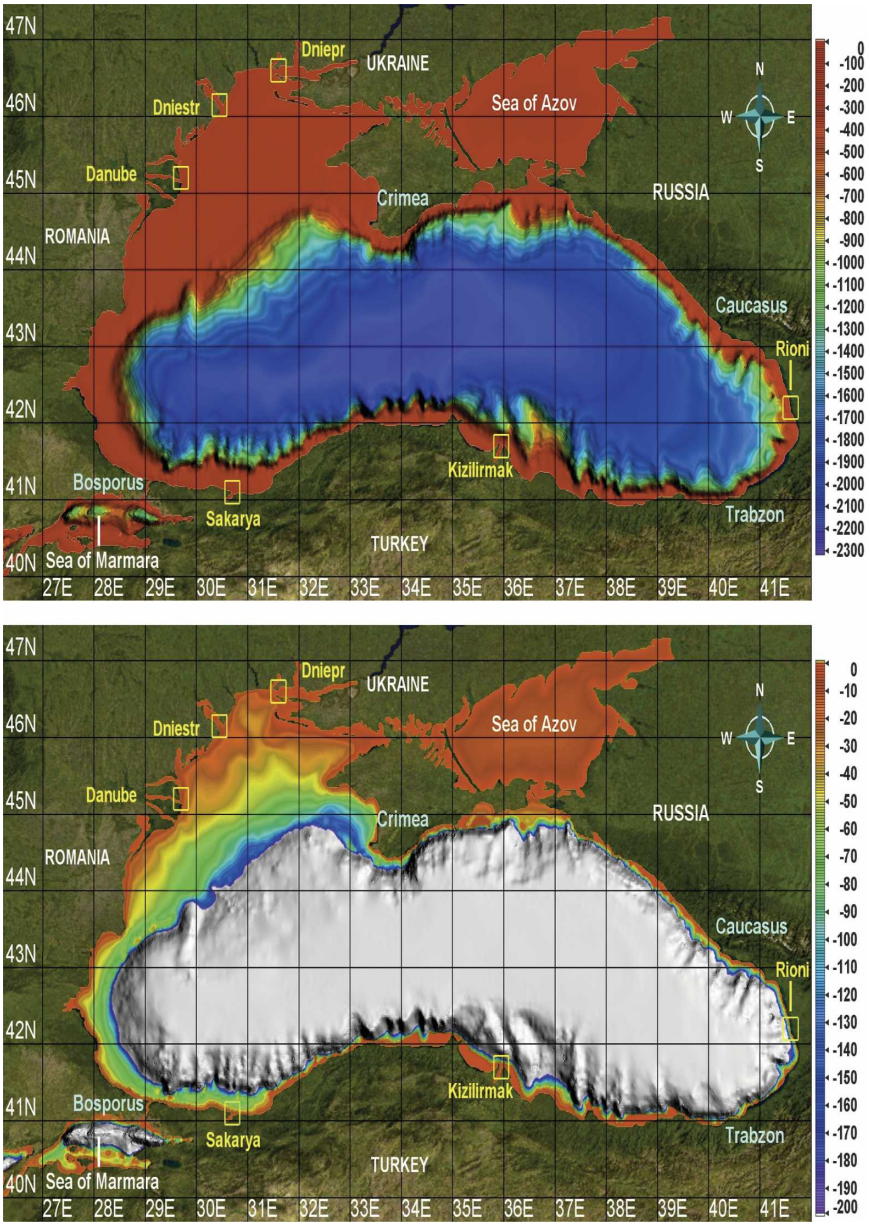

FIG. 1. The Black Sea bottom topography constructed from the 1-min DBDB-V resolution dataset of NAVOCEANO. Two different color bars are used to emphasize different depth ranges in the Black Sea: (top) deep water and (bottom) shallow water (< 200 m). Major rivers discharged into the Black Sea are in yellow. The land area map was produced using a subregion from the true color image of the National Aeronautics and Space Administration (NASA) earth observatory. Also shown are a few geographical locations mentioned in the text.

layer (e.g., Kara et al. 2005b), this gives us a basis for judging which of the simulations is better for this aspect (either annually or in seasons) and therefore, for deciding on optimal forcing products for SST in the Black Sea.

Although the atmospheric forcing fields and OGCM SST sensitivity to them is the primary focus, the sensitivity of the Black Sea mean surface circulation to different atmospheric wind stress products is also examined since the circulation is mainly wind driven (Oguz et al. 1995; Zatsepin et al. 2003). Specificially, the significant complexity of the Black Sea circulation (e.g., Staneva et al. 2001; Afanasyev et al. 2002; Zatsepin et al. 2003) is investigated using the eddy-resolving

TABLE 1. Atmospheric forcing sources (wind and thermal) that have been commonly used in previous Black Sea studies. Also included are data sources for initialization of temperature and salinity (*T*/*S*). Thermal forcing includes net shortwave radiation, net solar radiation (net shortwave plus net longwave radiation), air temperature, and air mixing ratio at 10 m above the sea surface. Some of the climatologies based on local datasets have coarse grid resolutions that may not be adequate for a small ocean basin, such as the Black Sea. Only a few Black Sea model studies used a model product (only NCEP) as atmospheric forcing (e.g., Stanev et al. 1997; Staneva et al. 2001), and Stanev et al. (2003) later used wind and thermal forcing parameters from the atmospheric analyses of the UKMO, demonstrating the accuracy of the latter in comparison to NCEP.

Wind forcing	Thermal forcing	*T*/*S* initialization
Sorkina (1974)	Makerov (1961)	Altman et al. (1987)
Hellerman and Rosenstein (1983)	Sorkina (1974)	Stanev (1990)
Rachev et al. (1991)	Golubeva (1984)	Trukhchev and Demin (1992)
NCEP 1000 mb (1980–86)	NCEP 1000 mb (1980–86)	
UKMO meteorolgoical data (1991–94)	Altman and Kumish (1986)	
Staneva and Stanev (1998)	Efimov and Timofeev (1990)	
	Stanev (1990)	
	Simonov and Altman (1991)	
	Golubev and Kuftarkov (1993)	
	UKMO Meteorological data (1991–94)	
	Staneva and Stanev (1998)	

OGCM in an attempt to mitigate the sparseness of observational data for evaluation of surface circulation features and the associated current speed and direction. One of our major purposes in writing this paper is to recommend to the Black Sea modeling community which wind and thermal forcing climatologies are reasonable and which ones should be avoided in simulating SST and circulation features in the Black Sea.

This paper is organized as follows. Section 2 describes atmospheric forcing fields in the Black Sea, along with a brief comparison between atmospheric forcing used in previous OGCM studies and those used here, several for the first time in the Black Sea. Section 3 gives general characteristics of the primitive equation, eddy-resolving OGCM used in this study. Section 4 discusses differences in model SST simulations, when the model is forced with various forcing fields formed from observation-based climatologies and operational model products, along with the impact of high-frequency versus monthly mean wind forcing on the simulations. Section 5 investigates the sensitivity of modeled Black Sea surface circulation to eight different wind stress products. Finally, section 6 gives the summary and conclusions of this paper.

2. Climatological atmospheric forcing in the Black Sea

Most previous Black Sea OGCM studies (e.g., Oguz et al. 1995; Oguz and Malanotte-Rizzoli 1996; Stanev and Beckers 1999; Staneva et al. 2001) made use of atmospheric forcing formed from local datasets, and those most commonly used are summarized in Table 1. Some of these data sources (e.g., Altman and Kumish 1986; Altman et al. 1987; Efimov and Timofeev 1990) are not documented in English or are not readily available. Through a detailed analysis, this section presents alternative sources for atmospheric forcing fields. In particular, the forcing products are constructed from operational model outputs and other observation-based climatologies, most of which have not been used in earlier Black Sea studies.

a. Candidate atmospheric forcing sets

Atmospheric forcing fields covering the Black Sea are formed from eight different products. Table 2 shows these products, along with their abbreviations used throughout the text. All atmospheric forcing fields were obtained in the form of global climatologies on the grid provided, and most are available online. Specifically, European Centre for Medium-Range Weather Forecasts: 10 m (EC10m), European Centre for Medium-Range Weather Forecasts: 1000 mb (EC1000), Navy Operational Global Atmospheric Prediction System (NOGAPS), and the National Centers for Environmental Prediction (NCEP) are climatologies formed from operational or reanalyzed model products, while the SeaWinds Scatterometer on Quick Scatterometer (QuikSCAT) satellite (SCAT), Comprehensive Ocean–Atmosphere Data Set (COADS), Southampton Oceanography Centre (SOC), and Hellerman–Rosenstein (HR) are climatologies based mainly on observational data. The grid resolution of these global climatologies varies from 0.25° to 2.5° (Table 3). A brief description of each dataset is given below.

EC10m, EC1000, and NCEP are all reanalyses that used a consistent data assimilation scheme and atmospheric forecast model; therefore, they are unaffected by operational model upgrades. The reanalyses from

TABLE 2. Abbreviations for the wind and thermal forcing products for the Black Sea as used throughout the text. Also included are the Web addresses from which each product was obtained. The Web addresses may be subject to changes by the originators. Operational products can be obtained from the National Center for Atmospheric Research (NCAR) data support section, and the NCAR dataset number is provided to clarify the products used in this paper. The interested reader is referred to the NCAR Web site given in the table to learn more about each dataset. Observation-based climatologies can be obtained from the Lamont-Doherty Earth Observatory, Columbia University, Web site. There are also other Web sites providing these datasets. All operational models have different boundary layer parameterizations, physics, data assimilation methods, and different satellite data used in the assimilations. Therefore, differences in their wind stress or surface flux outputs are expected. It should be emphasized that while the strength of operational products is that they provide gridded data with high temporal resolution, systematic errors of the assimilation model clearly influence analyses in data-sparse regions such as the Black Sea.

Acronym	Name of the wind dataset
EC10m	European Centre for Medium-Range Weather Forecasts, 10m (http://dss.ucar.edu/datasets/ds115.3/)
EC1000	European Centre for Medium-Range Weather Forecasts, 1000 mb (http://dss.ucar.edu/datasets/ds115.1/)
NOGAPS	Fleet Numerical Meteorology and Oceanography Center (http://usgodae.fnmoc.navy.mil/)
NCEP	National Centers for Environmental Prediction (http://dss.ucar.edu/datasets/ds090.0/)
SCAT	SeaWinds Scatterometer on QuikSCAT Satellite (http://www.coaps.fsu.edu/scatterometry)
COADS	Comprehensive Ocean–Atmosphere Data Set (http://iridl.ldeo.columbia.edu/SOURCES/.DASILVA/.SMD94/)
SOC	Southampton Oceanography Centre (http://ingrid.ldeo.columbia.edu/SOURCES/.SOC/.GASC97/)
HR	Hellerman–Rosenstein climatology (http://iridl.ldeo.columbia.edu/SOURCES/.HELLERMAN/)

these three products also overlap in time, and a common time interval (1979–93) has been chosen to form a climatology (Table 3). The common interval eliminates potential differences associated with the sampling period, and the 15-yr length (1979 to 1993) is sufficient to produce a reasonable climatology. Unfortunately, NOGAPS data do not extend to these earlier years, so we were limited to use data from 1990 to 2002 to form a climatology. As to observation-based climatologies, COADS is considered the most extensive collection of surface marine data available for the World Ocean. The purpose of creating the SOC climatology was to eliminate some of the biases in wind and other flux-related fields that existed in the COADS climatology (Josey et al. 1999). The observational data in the HR climatology cover a 106-yr period and were grouped by month into $2^\circ \times 2^\circ$ latitude–longitude boxes.

In addition to the climatologies mentioned above, we introduce a remotely sensed data source (hereinafter referred to as SCAT) based on the scatterometer [*Seasat*, *ERS-1/2*, NASA Scatterometer (NSCAT), and SeaWinds] observations of wind speed and direction over the ocean surface (e.g., Bourassa et al. 2003) to form a wind stress climatology over the Black Sea. Scatterom-

TABLE 3. Time interval during which each climatology was formed and grid resolutions for the atmospheric forcing products. Only thermal forcing from NOGAPS and EC10m is used. Thermal forcing from NCEP is not used in the HYCOM simulations, as it has relatively coarse grid resolution (1.875°) for the Black Sea. Availability of thermal forcing from NOGAPS starts in 1998. Operational model products provide relatively high-frequency atmospheric forcing (6 h), while observation-based climatologies have data collected at different times and days of a given month. The original ERA-15 used a model with a T106 spectral resolution. These data are distributed on an N80 Gaussian grid. Longitudinal resolution of EC10m, as used in this paper, is 1.125° but is only approximately this resolution in latitude. The EC1000 dataset was truncated to T47 (3.8°) along the equator and then interpolated to a 2.5° spherical grid. The winds from EC1000 are at a nominal height of 106 m. Thus they are adjusted to 10 m for use as atmospheric forcing. The archived grid resolution for the atmospheric forcing parameters from NOGAPS is 1.25° prior to 1998 and 1.0° since then. The combined NOGAPS wind stress climatology before/after 1997 was interpolated to a model grid and then merged for use. The NCEP reanalysis model has T62 spectral resolution. Data are distributed on either a 2.5° spherical or a Gaussian grid. On the Gaussian grid used here, the longitudinal resolution is 1.875° but is only approximately this resolution in latitude.

Dataset	Interval	Grid resolution	Time	Reference
EC10m	1979–93	$1.125^\circ \times 1.125^\circ$	6 h	Gibson et al. (1999)
EC1000	1979–93	$2.500^\circ \times 2500^\circ$	6 h	Gibson et al. (1999)
NOGAPS	1990–97	$1.250^\circ \times 1.250^\circ$	6 h	Rosmond et al. (2002)
NOGAPS	1998–2002	$1000^\circ \times 1000^\circ$		
NCEP	1979–93	$1.875^\circ \times 1.875^\circ$	6 h	Kalnay et al. (1996)
SCAT	1999–2002	$0.250^\circ \times 0.250^\circ$	12 h	Pegion et al. (2000)
COADS	1945–89	$1.000^\circ \times 1.000^\circ$	Monthly	da Silva et al. (1994)
SOC	1980–93	$1.000^\circ \times 1.000^\circ$	Monthly	Josey et al. (1999)
HR	1870–1976	$2.000^\circ \times 2.000^\circ$	Monthly	Hellerman and Rosenstein (1983)

eters are spaceborne radars that infer surface winds from the roughness of the sea surface as explained in Liu et al. (1998), and Liu (2002), in detail. Wind speed and direction are inferred from measurement of microwave backscattered power from a given location on the sea surface at multiple antenna look angles. Measurements of radar backscatter from a given location on the sea surface are obtained from multiple azimuth angles as the satellite travels along its orbit. Estimates of vector winds are derived from these radar measurements over a single broad swath of 1600-km width centered around the satellite ground track (e.g., Liu 2002). Scatterometer wind retrievals are calibrated to the neutral stability wind at a height of 10 m above the sea surface (Chelton et al. 2001). The SeaWinds scatterometer is an active microwave sensor that covers ≈90% of the ice-free ocean in one day, with an average of two observations per 25 km × 25 km grid cell each day. The gaps in the coverage are filled by using a variational method that minimizes a function with three constraints (Pegion et al. 2000). The functional term consists of misfits to the scatterometer observations, a penalty function to smooth with respect to a background field based on spatially smoothed scatterometer observations, and a misfit to the vorticity of the background field, which is a problem.

All data sources mentioned above are subject to their own unique biases. For example, errors and discrepancies exist in the observation-based climatologies because of varying quality and density of the input sources and changes in observing practices and data processing procedures throughout the history of data collection (e.g., Kent et al. 1993; Josey et al. 2002). Sampling error in the monthly SCAT winds is very small (e.g., Schlax et al. 2001). In operational atmospheric products, spurious trends may exist because of operational changes in the analysis/forecast system and changes in the input data stream as new data sources become available (e.g., Trenberth and Guillemot 1998).

b. Constructing wind and thermal forcing fields

For the Black Sea model, wind and thermal forcing parameters are formed from datasets discussed in section 2a. Wind forcing includes zonal and meridional wind stress magnitudes, and the total wind speed. Thermal forcing includes air temperature and air mixing ratio at 10 m above the sea surface, net shortwave radiation at the sea surface, and net solar radiation (net shortwave radiation plus net longwave radiation at the sea surface). Precipitation is also a thermal forcing parameter (see section 2d). Additional forcing parameters are a monthly climatological SST field for longwave radiation correction and a satellite-based ocean color climatology for attenuation of shortwave radiation (see section 3). The ocean model used in this paper reads in the time-varying wind and thermal atmospheric forcing fields.

Wind speed used for the model simulations is calculated from wind stress (Kara et al. 2002). By doing so, air–sea stability through the wind drag coefficient is taken into account, a consistent method for all wind stress products. Wind forcing products presented in this paper are unsmoothed in time, and a cubic spline is applied in space for interpolation to the model grid. Here, we first explain the methodology used to form wind stress from each product. Monthly mean wind stresses from NOGAPS, NCEP, COADS, and SOC are directly obtained from their original sources as surface stresses (N m^{-2}). Wind stress from HR is converted from dyn cm^{-2} to N m^{-2} using a scale factor of 0.1. Wind stresses from EC1000 and SCAT are obtained as pseudo stresses (m^2 s^{-2}), and they are later converted to surface stresses (N m^{-2}) by multiplying $\rho_{\text{air}} \times C_D$, where ρ_{air} is air density and C_D is variable wind drag coefficient. Here ρ_a at the air–sea interface is calculated using the ideal gas law formulation ($\rho_a = 100\ P_a/[R_{\text{gas}}(T_a + 273.16)]$ in kg m^{-3}), where T_a is air temperature (°C) at 10 m above the sea surface, R_{gas} is the gas constant with a value of 287.1 J kg^{-1} K^{-1} for dry air, and P_a is the atmospheric pressure at the sea surface with a value of 1013 mb. It is not necessary to consider a variable P_a in the density formulation because its effect on ρ_a is negligible in comparison to variations in T_a. Note that T_a values are taken from EC10m in this calculation for both products.

Wind stress (N m^{-2}) for EC10m is calculated using zonal and meridional wind velocities, T_a at 10 m above the sea surface, and SST, rather than using the surface stress product directly provided by ECMWF. The reason for not using the surface stresses is that they suffer from significant orographic effects near the coast. These result from Gibb's waves in the spectral model caused by the spectral truncation of the orography to 106 waves, triangular truncation (P. Kållberg, ECMWF, 2005, personal communication). They are most prominent in regions near steep mountains. After averaging fields originally created in the ECMWF spectral geometry, traces of the originally minute Gibb's waves become more visible, and after using the monthly means for certain derived parameters, such as the wind stress curl, they become even more prominent. On the other hand, the atmospheric variables in the EC10m product are from post-processed Businger profiles where the spectral traces have been removed. Thus, the use of surface stresses directly from the ECMWF model is not preferred. While NOGAPS provides atmospheric vari-

ables from which wind stress can be calculated, we use surface stresses directly from NOGAPS, which does not exhibit the Gibb's wave problem (e.g., Metzger 2003).

The wind stress calculation for EC10m uses bulk formulas that include a stability-dependent drag coefficient through air–sea temperature difference and temperature-dependent air density (Kara et al. 2002). Some OGCMs in the Black Sea have used wind stresses that are constructed from 10-m winds and a constant drag coefficient. For example, Oguz and Malanotte-Rizzoli (1996) used a drag coefficient value of 1.3×10^{-3}. However, such wind stresses exclude the significant changes in magnitude that can occur due to effects of wind speed and air–sea stability in the drag coefficient, which can make it quite variable. This becomes especially important for OGCMs that predict SST because air–sea stability depends mainly upon the air–sea temperature difference and wind speed. As noted above, the use of a bulk formula for wind stress can be more desirable when performing fine-resolution OGCM simulations than using the direct product from an operational model. While more advanced methods exist (e.g., Fairall et al. 2003; Bourassa et al. 2005), the bulk formula used here (Kara et al. 2002) for wind stress forcing of an OGCM with SST is generally accurate and computationally much more efficient.

We now present the spatial patterns of long-term annual mean wind speed (Fig. 2a). The basin-averaged NCEP wind speed has an annual mean of 4.6 m s^{-1}, the highest from the eight products (Table 4). Not surprisingly, the NCEP product (Table 3) is probably not a preferred product in the Black Sea because the wind speeds have relatively large differences in comparison to those from research vessel measurements (e.g., Smith et al. 2001; Josey et al. 2002). Wind speed from the finest-resolution dataset, SCAT, resolves many small-scale futures. In general, HR wind stresses tend to be strong over the global ocean because they were created using relatively large drag coefficients (Harrison 1989). The spatial patterns of annual mean wind stress curl from the eight products also differ substantially (Fig. 2b). In particular, wind stress curl from NCEP is rather large and from COADS and SOC rather small in comparison to the other products.

Climatologies of monthly mean thermal forcing parameters are constructed using 6-hourly (hereinafter referred to as 6-h) model output during 1979–93 for ECMWF, 1998–2002 for NOGAPS, and 1948–2003 for NCEP. Similar to the wind forcing, thermal forcing parameters are daily averages that are linearly interpolated to 6-h intervals. A cubic spline in space is applied to all thermal forcing parameters for interpolation to the model grid. Although thermal forcing fields from NCEP are presented for comparison purposes, they are not used in the model simulations. The main reason is that NCEP has rather coarse resolution (1.875° × 1.875°) for a small ocean basin, such as the Black Sea. In addition, atmospheric forcing from NCEP needs to be corrected before use in an OGCM because the means of thermal forcing parameters from NCEP are quite different in comparison to those from local climatological sets and those from the atmospheric analyses of the U.K. Met Office (UKMO) in the Black Sea (Staneva and Stanev 1998; Stanev et al. 2003). Previously, it was also shown that the oceanic response to very smooth NCEP forcing resulted in unrealistic simulations in the Black Sea (Stanev et al. 1997).

Thermal forcing parameters from EC10m, NOGAPS, and NCEP differ in the annual means (Fig. 2c). These differences can be partially attributed to the time intervals over which the climatologies were constructed: 1979–93 for EC10m and 1998–2002 for NOGAPS. Because no NOGAPS thermal forcing is available prior to 1998, we had to form the climatology based on only a 5-yr model output. A comparison between EC10m and NOGAPS over the same time period (1998–2002) gave better agreement (not shown). Annual mean air temperature from EC10m is colder than that from NOGAPS by ≈2°–4°C over the northernmost Black Sea, including the northwestern shelf and either side of the Crimean peninsula. This is an indication of the fact that, in addition to improper land–sea masks discussed in Kara et al. (2005b), the local orography can have a major effect on the accuracy of climatological fields constructed from operational model outputs. In most regions, the spatial pattern and magnitude of air temperature are generally similar for all three datasets. In addition, all three have usually similar spatial patterns for air mixing ratio at 10 m above the sea surface. The most obvious differences between EC10m, NOGAPS, and NCEP are seen in the shortwave and net solar radiation values (see also Table 4).

In addition to the annual mean, the seasonal cycle of the wind and thermal forcing fields is examined to determine if the annual mean is dominated by values in any specific season. There are relatively weak winds (≈2.5 m s^{-1}) in spring from April to June, and this is true for almost all products except NCEP and NOGAPS (Fig. 3). The basin-averaged climatological monthly mean speed given by a local dataset (Efimov and Timofeev 1990) reports values of 5 to 8 m s^{-1} from summer to winter, which is usually higher than the wind forcing products presented here. The remotely sensed SCAT data can be considered as a good measure of wind speed over the Black Sea as it was calculated from

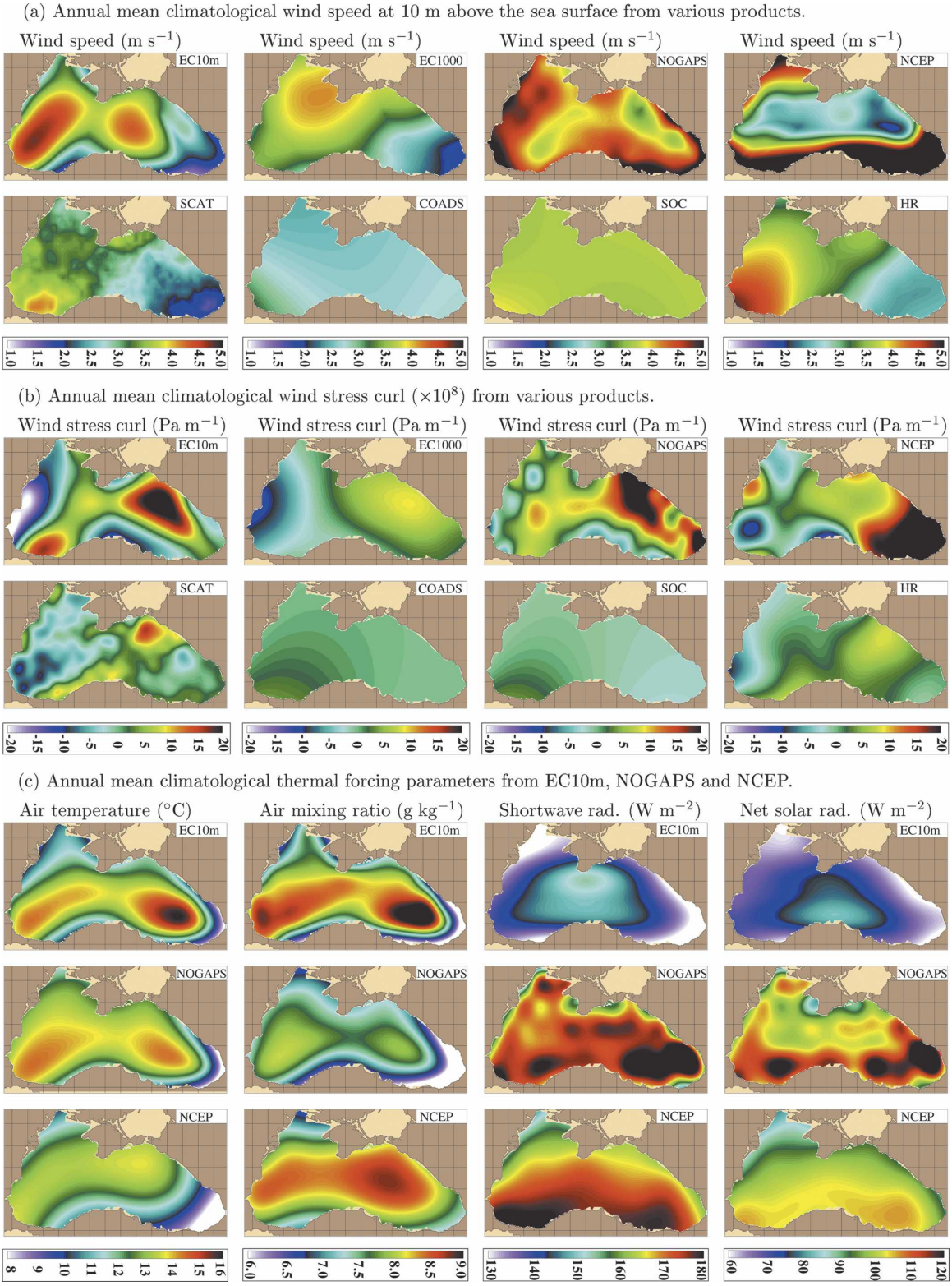

FIG. 2. Climatological annual mean of wind and thermal forcing parameters formed from observation-based climatologies and operational model outputs: (a) wind speed, (b) wind stress curl, and (c) thermal forcing from 15-yr ECMWF Re-Analysis (ERA-15), NOGAPS, and NCEP. In general, wind speed climatologies constructed from observations (COADS and SOC) are very smooth. The wind fields from NCEP reveal very different spatial patterns in comparison to other operational model products (i.e., EC10m, EC1000, and NOGAPS).

TABLE 4. Basin-averaged annual mean values of atmospheric forcing parameters in the Black Sea. Also given are min and max values in the annual mean fields. Std dev is calculated over the annual cycle using monthly mean values. The similarity based on different sources suggests that a basin-averaged annual mean value of ≈ 3 m s^{-1} is probably a good estimate for the Black Sea. Net shortwave and net solar radiation values from EC10m and NOGAPS are different by ≈ 30 W m^{-2}. Basin-averaged thermal forcing values from NCEP are included for only comparison purposes. The climatological relative bias values for air temperature, air mixing ratio, net shortwave radiation, and net solar radiation calculated for NOGAPS–EC10m (NCEP–EC10m) are 0.3°C (−0.8°C), −0.7 g kg^{-1} (0.2 g kg^{-1}), 32.8 W m^{-2} (29.9 W m^{-2}), and 36.2 W m^{-2} (29.9 W m^{-2}), respectively. Similarly, bias values for NOGAPS–NCEP are 0.9°C, −0.9 g kg^{-1}, 2.9 W m^{-2}, and 6.3 W m^{-2}.

Forcing product	Mean	Min	Max	Std dev
Wind speed (m s^{-1})				
EC10m	3.5	1.3	4.8	0.78
EC1000	3.4	1.9	4.2	0.82
NOGAPS	4.0	2.4	5.4	0.84
NCEP	4.6	2.6	8.5	0.96
SCAT	3.0	1.6	4.2	0.76
COADS	2.7	2.5	3.3	0.37
SOC	3.7	3.6	3.9	0.82
HR	3.4	2.4	4.9	0.63
Wind stress curl ($\times 10^8$) (Pa m^{-1})				
EC10m	2.6	−24.2	24.1	2.6
EC1000	1.4	−10.4	9.3	2.7
NOGAPS	6.3	−21.9	39.1	5.4
NCEP	8.0	−15.1	42.3	11.4
SCAT	0.9	−19.1	25.1	2.4
COADS	1.1	0.1	4.2	1.1
SOC	−0.1	−1.7	4.1	1.9
HR	2.2	−9.8	8.8	2.1
Air temperature (°C)				
EC10m	12.9	7.6	16.0	6.5
NOGAPS	13.2	6.9	14.6	6.5
NCEP	12.1	5.7	13.8	6.4
Air mixing ratio (g kg^{-1})				
EC10m	8.0	5.3	9.4	3.3
NOGAPS	7.3	4.7	8.1	2.9
NCEP	8.2	6.6	8.8	3.0
Shortwave radiation (W m^{-2})				
EC10m	141.3	122.2	154.1	77.6
NOGAPS	174.1	146.3	198.2	77.4
NCEP	171.2	148.4	184.5	79.8
Net solar radiation (W m^{-2})				
EC10m	71.4	58.0	84.1	75.1
NOGAPS	107.6	80.1	135.0	81.2
NCEP	101.3	80.0	107.4	77.2

calibrated wind speed and direction measurements of the SeaWinds scatterometer on the QuikSCAT satellite. The available record of QuickSCAT winds used in this paper is from August 1999 through March 2002. Although this time period (2.5 yr) is relatively short to represent the climatological conditions, the SCAT climatology has the advantage of providing fine spatial resolution. The differences existing in wind speed are also reflected in the wind stress curl (Fig. 4). Wind stress curl from NCEP is too large, and previously Schrum et al. (2001) also noted unrealistic wind stress curl from NCEP in the Black Sea but used fields constructed over a different time period from that used here. They note that the amplitude of the seasonal cycle based on the EC10m data is very different than that estimated from the NCEP data, but the wind stress curl from EC10m is comparable to estimates from local climatic data and higher-resolution UKMO data over 1993–96.

There is a strong seasonal cycle in all thermal forcing parameters (Fig. 5). Using the local datasets, Staneva and Stanev (1998) reported basin-averaged air temperatures of ≈5°C in January and February, which agrees with those from EC10m, NOGAPS, and NCEP. Basin-averaged net solar radiation values shown in Fig. 3a of Oguz and Malanotte-Rizzoli (1996), as determined from local climatologies, are roughly 15, 40, and 85 W m^{-2} in January, February, and March and 190, 210, and 200 W m^{-2} in May, June, and July, respectively. These values are larger than those obtained from EC10m. Interestingly, Oguz and Malanotte-Rizzoli (1996) indicated that original flux values based on local datasets, as used in their model simulations, are probably too large in winter, and slightly larger (e.g., 10 to 30 W m^{-2}) in summer, resulting in unrealistic temperature simulations. This partly demonstrates the reliability of net solar radiation values from EC10m in comparison to the local datasets. The most striking feature of monthly mean thermal forcing parameters in the Black Sea is that net shortwave radiation from EC10m is consistently lower than that from NOGAPS and NCEP by an offset of ≈30 W m^{-2} in all months (Fig. 6). Such a difference can change the amount of net flux that penetrates to depth, especially during summer when very thin mixed layers are present in the Black Sea (Kara et al. 2005a).

c. *Addition of a high-frequency component*

There are two main reasons for adding a high-frequency component to monthly mean atmospheric forcing fields: 1) the mixed layer is sensitive to variations in surface forcings on time scales of a day or less (e.g., Kelly et al. 1999; Sui et al. 2003; Wallcraft et al. 2003; Kara et al. 2003; Stanev et al. 2004), and 2) our future goal is to perform simulations forced by high-frequency interannual atmospheric fields from operational weather centers.

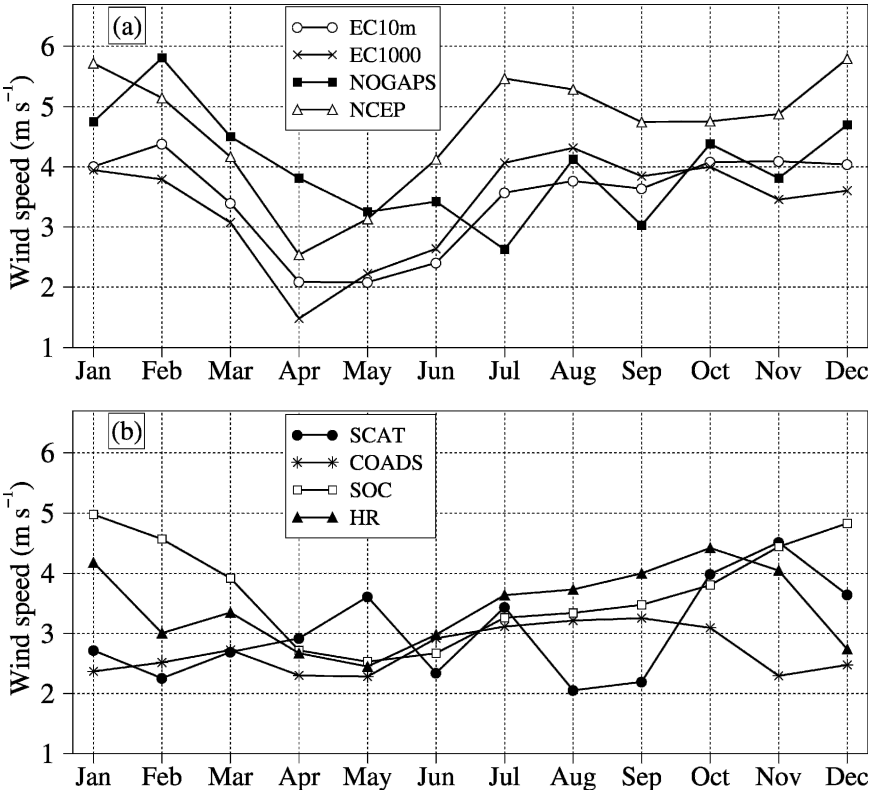

FIG. 3. Basin-averaged monthly mean wind speed obtained from (a) operational model products (upper group) and (b) observation-based climatologies (lower group). Note that scatterometers are spaceborne radars that infer surface winds from the roughness of the sea surface, and the available record of SCAT winds used in this paper is from Aug 1999 through Mar 2002. Wind speeds from operational products commonly demonstrate large differences, while the observation-based wind climatologies usually agree better with each other.

Hybrid winds consist of monthly winds from each product plus EC10m intramonthly wind anomalies. The first step for creating hybrid winds is to take the monthly climatologies from each wind product (see Table 3) and perform a 6-h linear interpolation between the monthly values. The intramonthly EC10m anomalies interpolated to the product grid are added to EC10m, EC1000, NOGAPS, NCEP, SCAT, COADS, SOC, and HR, separately, to form hybrid wind products to be used in ocean model studies.

Construction of the EC10m hybrid winds is briefly described here. The same procedure is applied to other products. For the OGCM wind stress forcing, 6-h intramonthly anomalies from EC10m are used in combination with the monthly mean wind stress climatology of EC10m interpolated to 6-h intervals. The 6-h anomalies are obtained from a reference year. For this purpose, the winds from September 1994 through September 1995 (6 h) are used because they represented a typical annual cycle of the EC10m winds, and because the September winds in 1994 and 1995 most closely matched each other. The 6-h September 1994 and September 1995 wind stresses are blended to make a complete annual cycle, which is denoted by $\boldsymbol{\tau}_{\mathrm{EC10m}}$. The wind stresses are calculated from EC10m winds using the bulk formulas of Kara et al. (2002), as mentioned above. Monthly averages are first formed from the September 1994 through September 1995 EC10m wind stresses ($\boldsymbol{\tau}_{\mathrm{EC10m}}$). These are then linearly interpolated to the time intervals of the 6-h EC10m winds to produce a wind stress product ($\boldsymbol{\tau}_I$). The anomalies are then obtained by applying the difference ($\boldsymbol{\tau}_A = \boldsymbol{\tau}_{\mathrm{EC10m}} - \boldsymbol{\tau}_I$). Scalar wind speed is obtained from the input wind stress and therefore has 6-h variability. Note that other products provide surface stress directly so the high-frequency component ($\boldsymbol{\tau}_A$) is added to the interpolated monthly mean wind stress directly.

d. Evaporation and precipitation

The Black Sea model simulations presented in this paper are carried out in a closed basin configuration. Thus, the excess of precipitation and river runoff over

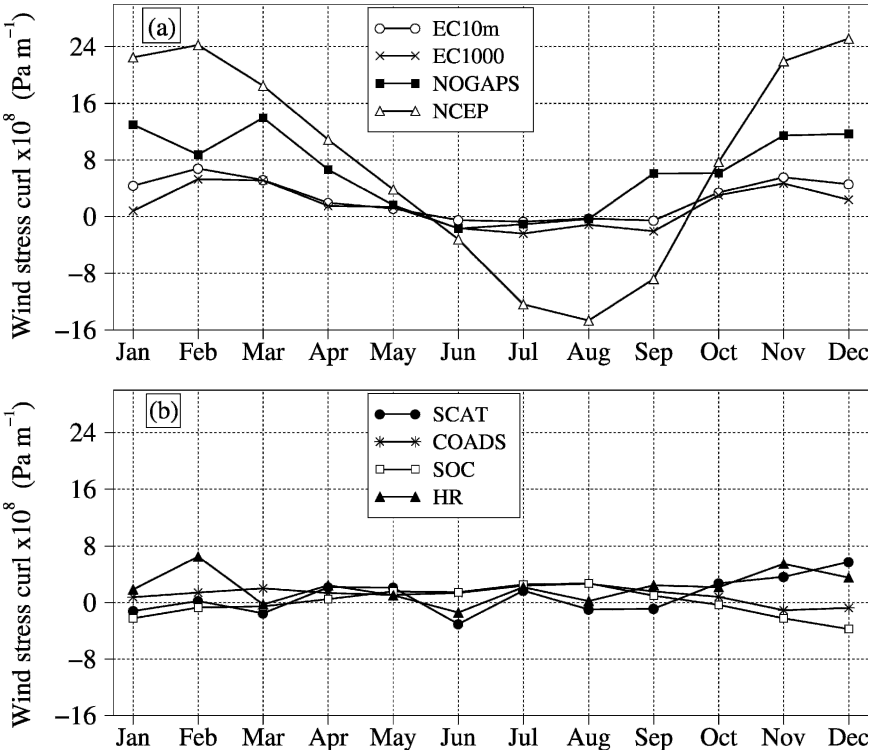

FIG. 4. Basin-averaged monthly mean wind stress curl obtained from (a) operational model products and (b) observation-based climatologies. It should be emphasized that wind stress curl from NCEP is substantially larger than that from other products. A comparison of wind stress curl from the NCEP reanalysis (1948–2003) to one from the NCEP data used in this paper (1979–93) revealed almost identical patterns and magnitudes (not shown), demonstrating that the time period used for constructing the climatology is not the reason for seeing large wind stress.

evaporation must be removed, leading to a zero balance in the Black Sea. The net freshwater balance (P_{net}) in the Black Sea model is expressed as $P_{\text{net}} = E + P + P_{\text{River}} + P_{\text{Bosp.}}$, where E is evaporation, P is inflow precipitation due to rain or snow, P_{River} is inflow input as an equivalent volume of precipitation, and $P_{\text{Bosp.}}$ is outflow treated as negative precipitation due to the net southward transport through the Bosporus Strait. The model treats a total of six major rivers shown in Fig. 1 as a "runoff" addition to the surface precipitation field, and the Bosporus Strait as a negative river precipitation (i.e., a river evaporation) to close freshwater flux balance. The monthly mean river discharge values are taken from Vörösmarty et al. (1997), whose annual mean values usually agree with those reported by Perry et al. (1996). As expected, P_{net} would not be zero because there are rivers, having small discharge values, which are not used in model simulations. The small net bias is made up with a precipitation offset in the model simulations, leading to a zero freshwater flux within the basin.

Here, the focus is to examine E and P values obtained from EC10m, NOGAPS, and NCEP (Fig. 7) and to compare them with values reported in earlier studies. Evaporation values are directly calculated from latent fluxes from EC10m, NOGAPS, and NCEP to be consistent with evaporation estimates from local datasets. The monthly mean E values are estimated using $E = Q_L/(\rho_w L)$, where Q_L is latent heat flux (W m^{-2}), ρ_w is water density (1022 kg m^{-3}), and L is latent heat of vaporization [$L = (2.501 - 0.00237 \times \text{SST})10^6$ J kg^{-1}] with SST obtained from EC10m, NOGAPS, and NCEP. Basin-averaged annual mean E values for EC10m, NOGAPS, and NCEP are ≈ -270, -266, and -335 km^3 yr^{-1}, respectively (Fig. 8a). Unluata et al. (1990) provided an estimate of 350 km^3 yr^{-1} for E and 300 km^3 yr^{-1} for P, which are very large in comparison to those obtained from EC10m and NOGAPS. The agreement in E values from EC10m and NOGAPS is due to the agreement in latent heat fluxes from these two models (not shown).

Using the Sevastopol Marine Data Information As-

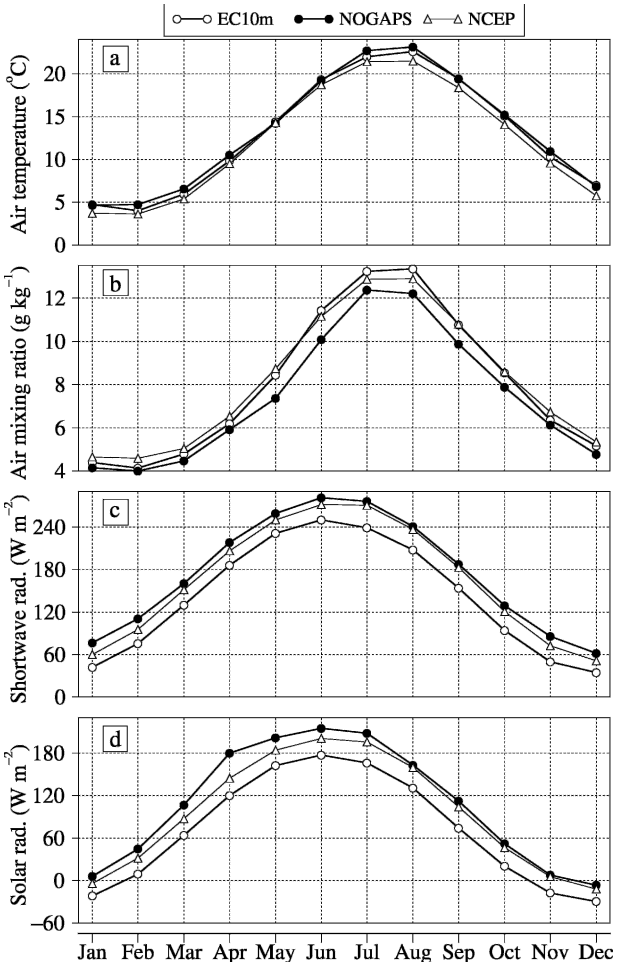

FIG. 5. Basin-averaged monthly mean thermal forcing parameters obtained from EC10m, NOGAPS, and NCEP: (a) air temperature at 10 m above the sea surface, (b) air mixing ratio at 10 m above the sea surface, (c) net shortwave radiation at the sea surface, and (d) net solar radiation, which is the sum of net shortwave radiation and net longwave radiation at the sea surface. All of these parameters are directly formed from the 6-h outputs of three operational models over the Black Sea. The rms difference values calculated over the annual cycle (cf. section 4) for air temperature, air mixing ratio, net shortwave radiation, and net solar radiation between EC10m and NOGAPS (NCEP) are 0.5°C (0.8°C), 0.8 g kg^{-1} (0.4 g kg^{-1}), 33.0 W m^{-2} (30.4 W m^{-2}), and 37.4 W m^{-2} (29.2 W m^{-2}), respectively. Similarly, those between NCEP and NOGAPS are 1.1°C, 0.9 g kg^{-1}, 4.8 W m^{-2}, and 11.4 W m^{-2}.

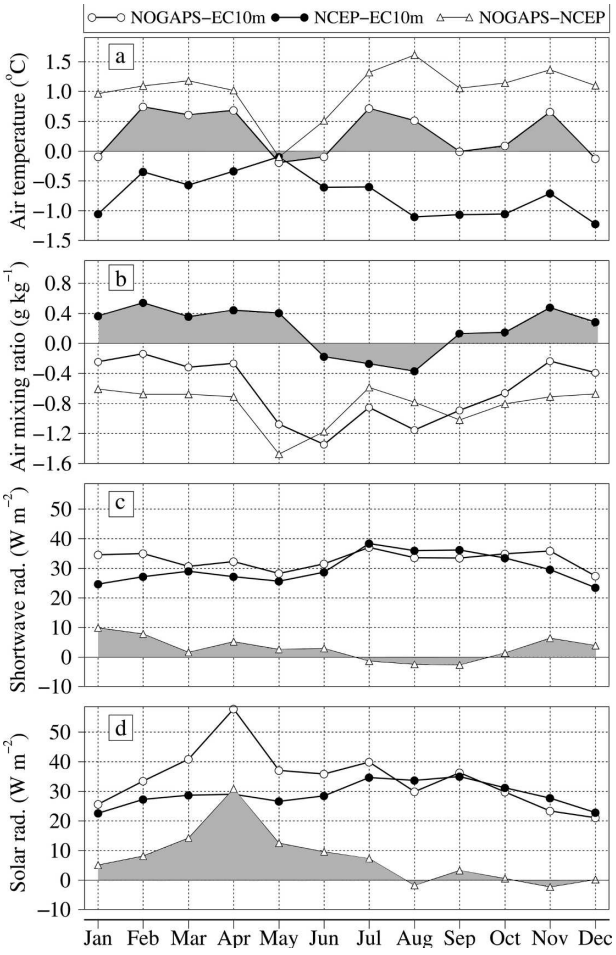

FIG. 6. Same as in Fig. 5, but for monthly mean differences between thermal forcing parameters. Some of the differences are attributed to fact that the climatology from NOGAPS output was formed using 5 yr of model output (1998–2002), which is the only available time period as of this writing, while a 15-yr period of model output (1979–93) was used to obtain the climatology from EC10m and NCEP. This was confirmed from climatologies constructed using the same time period (1998–2002), which did not show significant differences.

sociation (SMDIA) data for the Black Sea, Oguz et al. (1995) gave a climatological annual mean E of 384 km^3 yr^{-1} in their OGCM study, a value which is ≈110 km^3 yr^{-1} greater than those obtained from EC10m and NOGAPS. In addition, based on observational local datasets (Efimov and Timofeev 1990; Stanev 1990), basin-averaged E reaches its maximum with a value of ≈−150 mm month^{-1} (740 km^3 yr^{-1}) in August (see Fig. 4a of Oguz and Malanotte-Rizzoli 1996), which is also true for NOGAPS with one-month delay (i.e., September) for EC10m and NCEP. However, this maximum E value is almost twice as large as EC10m (≈−80 mm month^{-1} or −392 km^3 yr^{-1}), NOGAPS (≈−84 mm month^{-1} or −413 km^3 yr^{-1}), and also larger than that of NCEP (≈−108 mm month^{-1} or −533 km^3 yr^{-1}). All of these analyses demonstrate that the largest values are from SMDIA, giving an overestimation in E in comparison to EC10, NOGAPS, and NCEP. The uncertainty in E is not surprising at all since knowledge of the annual and interannual variability of the moisture flux is rather limited in many regions of the global ocean because of the lack of available in situ measurements,

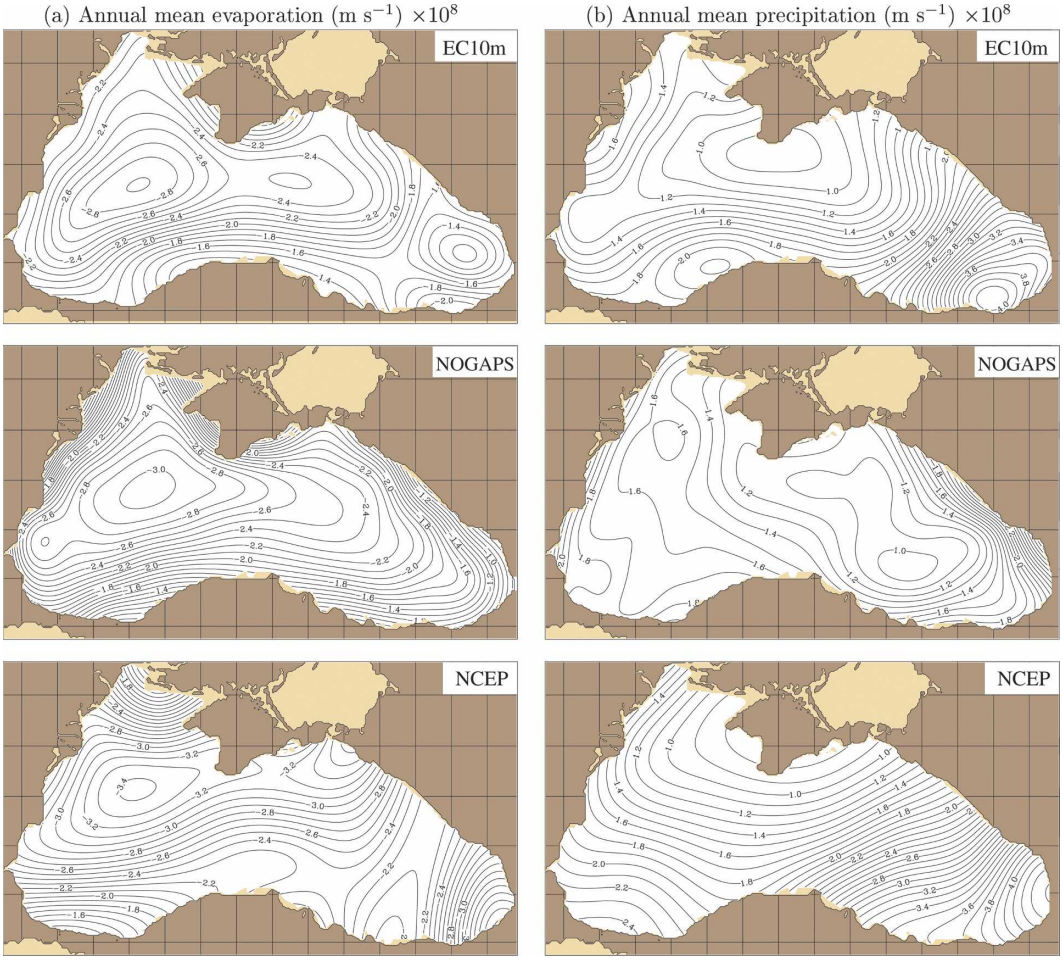

FIG. 7. Spatial fields of climatological annual mean of (a) evaporation and (b) precipitation. They are all in m s^{-1} and are scaled by $\times 10^8$. In the panels, the "+" sign indicates a gain to ocean, and the "−" sign indicates a loss from ocean. The unit conversions can be made using 1 m s^{-1} = $10^3 \times 30 \times 24 \times 60 \times 60$ mm month^{-1} and 1 m s^{-1} = $10^{-3} \times 365 \times 24 \times 60 \times 60$ km yr^{-1}.

causing incorrect latent heat flux estimations and thus evaporation on various time scales (e.g., Weare 1989; Kent and Taylor 1995; Gleckler and Weare 1997). There are also significant errors in satellite estimations of the latent heat flux (e.g., Bourras et al. 2002; Jo et al. 2004).

Basin-averaged annual mean P values are 221, 188, and 255 km^3 yr^{-1}, clearly demonstrating uncertainities among EC10m, FMMOC, and NCEP (Fig. 8b). Although precipitation measurements are sparse (mainly from ship observations) in the Black Sea, monthly mean climatological precipitation based on local datasets usually agrees with those from EC10m, FMMOC, and NCEP. For example, the basin-averaged annual mean precipitation values reported from local datasets are 45.0 mm month^{-1} or ≈222 km^3 yr^{-1} (Makerov 1961) and 47.9 mm month^{-1} or ≈236 km^3 yr^{-1} (SMDIA data). The latter dataset includes 20 more years of data than the former one, resulting in some differences. Oguz et al. (1995) also used an annual mean P value of ≈226 km^3 yr^{-1} in the model simulations. While the P values reported from local datasets roughly agree with the value reported from EC10m (≈221 km^3 yr^{-1}), they are significantly larger/smaller than the NOGAPS/NCEP estimates. The largest P estimate in the Black Sea appears to be ≈300 km^3 yr^{-1} by Unluata et al. (1990).

In summary, an examination of the freshwater flux balance in the Black Sea reveals that rivers provide ≈287 km^3 yr^{-1}, precipitation accounts for ≈220 km^3 yr^{-1}, evaporation removes ≈270 km^3 yr^{-1}, and outflow through the Bosporus is ≈217 km^3 yr^{-1} (not shown here). For these calculations, a total of six major rivers (Danube, Dniepr, Dniestr, Rioni, Sakarya, and Kizilirmak) are considered. The total discharge from these six major rivers into the Black Sea is ≈287 km^3 yr^{-1}. Pre-

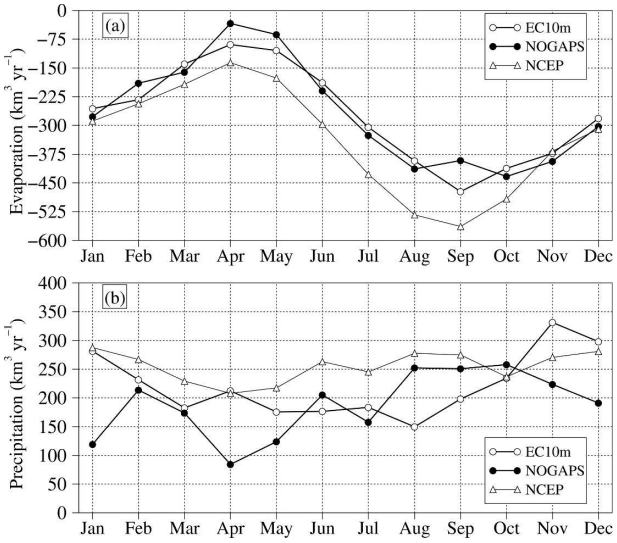

FIG. 8. Basin-averaged monthly mean values for (a) evaporation and (b) precipitation. They were both obtained in m s^{-1} and converted to km^3 yr^{-1}. Although evaporation is calculated in the model (i.e., it is not a prescribed forcing) using simulated latent heat flux at each time step, it is shown here for comparison. Monthly mean precipitation fields that are linearly interpolated to 6-h intervals are directly read into the model in m s^{-1}. The climatological annual mean evaporation (precipitation) bias values are 4.4 (−33.5), −65.0 (33.6), and 69.4 (−67.1) km^3 m^{-1} for NOGAPS–EC10m, NCEP–EC10m, and NOGAPS–NCEP, respectively. The rms difference values calculated over the annual cycle (cf. section 4) for evaporation (precipitation) are 37.3 (83.7), 78.2 (59.7), and 88.2 (82.3) km^3 m^{-1} between the pairs of NOGAPS and EC10m, NCEP and EC10m, and NOGAPS and NCEP. Similarly, linear correlation coefficients are 0.96 (0.01), 0.95 (0.40), and 0.92 (0.49) for the same pairs, indicating that monthly mean evaporation from all three products have similar seasonal cycles, while this is not true for the precipitation.

cipitation and evaporation estimates are based on the EC10m data. Bosporus outflow values are taken from Fig. 7b of Staneva and Stanev (1998).

3. HYCOM description

The Hybrid Coordinate Ocean Model (HYCOM) is based on primitive equations (Bleck 2002). It contains five prognostic equations: two for the horizontal velocity components, a mass continuity or layer thickness tendency equation, and two conservation equations for a pair of thermodynamic variables, such as salt and temperature or salt and density.

HYCOM behaves like a conventional σ (terrain following) model in very shallow oceanic regions, like a z-level coordinate model in the mixed layer or other unstratified regions, and like an isopycnic-coordinate model in stratified regions. However, the model is not limited to these coordinate types (Chassignet et al. 2003). The model has several mixed layer/vertical mixing options, which are discussed and evaluated in Halliwell (2004). In this paper, we use the nonslab K-Profile Parameterization (KPP) of Large et al. (1997).

The net surface heat flux that has been absorbed (or lost) by the upper ocean to depth is parameterized as the sum of the downward surface solar irradiance, upward longwave radiation, and the downward latent and sensible heat fluxes. The amount of net shortwave radiation that enters the mixed layer depends on the solar attenuation depths, which can significantly influence upper open variables in the Black Sea simulations (Kara et al. 2005c). Thus, the effect of turbidity on solar radiation penetrating to depth is accounted for by using a monthly attenuation of photosynthetically available radiation (k_{PAR}) climatology over 1997–2001. These satellite-based climatological k_{PAR} fields are derived from Sea-Viewing Wide Field-of-View Sensor (SeaWiFS) data on the spectral diffuse attenuation coefficient at 490 nm (k_{490}) and have been processed to have smoothly varying and continuous coverage (Kara et al. 2004).

Latent and sensible heat fluxes at the air–sea interface are calculated using efficient and computationally inexpensive bulk formulas that include the effects of dynamic stability (Kara et al. 2002). Our experience with the model simulations confirms that the surface heat flux forcing causes the model SST to relax toward an equilibrium state prescribed by the air temperature and air mixing ratio climatologies. Thus, it is reasonable to expect successful HYCOM simulations of SST by letting the model calculate its own surface heat fluxes including effects of atmospheric stability via exchange coefficients. Net solar radiation at the sea surface is so dependent on cloudiness that it is taken directly from ECMWF (or NOGAPS) for use in the model. Basing fluxes on the model SST automatically provides a physically realistic tendency toward the correct SST (Wallcraft et al. 2003). A longwave radiation correction is applied in the form of a relaxation term (Kara et al. 2005b).

The Black Sea model setup is explained in Kara et al. (2005b) in detail. The model has a resolution of 1/25° × 1/25° cos(lat), (latitude × longitude) (≈3.2 km). There are a total of 15 hybrid layers (10 predominantly isopycnal and 5 always σ or z levels). The model has isopycnal coordinates in the stratified ocean but uses the layered continuity equation to make a dynamically smooth transition to z levels (fixed-depth coordinates) in the unstratified surface mixed layer and σ levels (terrain-following coordinates) in shallow water. The optimal coordinate is chosen every time step using a hybrid coordinate generator. Thus, HYCOM automatically

TABLE 5. A description of 16 climatologically forced HYCOM simulations used in this paper. The reader is referred to the text for construction of each atmospheric forcing product. River forcing is considered under the thermal forcing. The model array size is 360 × 206, and performing a 1-month simulation takes ≈0.7 wall-clock hours using 64 HP/COMPAQ SC45 processors at the U.S. Army Engineer Research and Development Center (ERDC). The model is run until it reaches statistical equilibrium using climatological monthly mean thermal atmospheric forcing, but with wind forcing that includes the 6-h variability as explained in the text. It takes about 5–8 model years for a simulation to reach statistical equilibrium for all model parameters. The model is deemed to be in statistical equilibrium when the rate of potential energy change is acceptably small (e.g., < 1% in 5 yr) in all layers.

HYCOM simulation	Wind forcing	Thermal forcing	HYCOM simulation	Wind forcing	Thermal forcing
Expt 1	EC10m	EC10m	Expt 9	EC10m	NOGAPS
Expt 2	EC1000	EC10m	Expt 10	EC1000	NOGAPS
Expt 3	NOGAPS	EC10m	Expt 11	NOGAPS	NOGAPS
Expt 4	NCEP	EC10m	Expt 12	NCEP	NOGAPS
Expt 5	SCAT	EC10m	Expt 13	SCAT	NOGAPS
Expt 6	COADS	EC10m	Expt 14	COADS	NOGAPS
Expt 7	SOC	EC10m	Expt 15	SOC	NOGAPS
Expt 8	HR	EC10m	Expt 16	HR	NOGAPS

generates the lighter isopycnal layers needed for the pycnocline during summer. These become z-levels during winter. The density values for the isopycnals and the decreasing change in density with depth between isopycnal coordinate surfaces are based on the density climatology from the Modular Ocean Data Assimilation System (MODAS; Fox et al. 2002). HYCOM is initialized using temperature and salinity profiles from the MODAS climatology. The Black Sea bottom topography (Fig. 1) was formed from the 1-min Digital Bathymetric Database-Variable (DBDB-V) resolution dataset, which also includes river bathymetry, obtained from the Naval Oceanographic Office (NAVOCEANO). Lighting (shading) in the bathymetry is intended to show detailed features of canyons, shelf break areas, and mountain ranges.

4. The impact of atmospheric forcing on the model SST simulations

Climatologically forced HYCOM simulations (Table 5) are performed to examine the sensitivity of SST to the choice of atmospheric forcing products for SST. During the model integration, there is no assimilation of any oceanic data except for relaxation to sea surface salinity (SSS) from the MODAS climatology. The model is initialized using temperature and salinity from the MODAS climatology. The nominal e-folding time for the SSS relaxation is 30 days, assuming a constant mixed-layer depth (MLD) of 30 m. The actual e-folding time depends on the mixed layer depth and is $30 \times 30(\text{MLD})^{-1}$ days, that is, it is more rapid when the MLD is shallow and less so when it is deep. The wind forcing includes monthly mean wind stresses with the addition of high-frequency components as explained in section 2c.

For evaluation of the model results, monthly mean SSTs are formed from daily fields using the last 4 model years (years 5 through 8). At least a 4-yr mean was needed because HYCOM with 3.2-km resolution has a strong nondeterministic component due to flow instabilities. These are a major contribution to the simulated Black Sea circulation at this resolution. Monthly mean HYCOM SST fields are then compared to climatological SST fields at each model grid point. Our main goal is not only to investigate which atmospheric forcing product gives the best Black Sea simulation, but also to determine which one yields a better simulation near land/sea boundaries or in the interior.

a. HYCOM evaluation

The climatological SST (truth) used here is the Pathfinder dataset, which is based directly on satellite measurements (Casey and Cornillon 1999). The monthly climatology covers 1985–97, and it has a resolution of ≈9.3 km. Both daytime and nighttime daily SST values are included in each monthly average. A 7×7 median smoother box filter was applied to remove small-scale noise, replacing each pixel with the median of the pixels in the surrounding 7×7 pixel box, effectively yielding spatial resolution of ≈30 km. The final monthly mean Pathfinder SST climatology was also smoothed 7 times to get rid of the blocky SST variability found in the original data source. The Pathfinder climatology is preferred for the model–data comparisons as it outperforms the commonly used climatologies (Casey and Cornillon 1999), and it also has much finer resolution than the others, which is appropriate for the fine-resolution Black Sea model used in this paper.

Several statistical measures are considered to assess the strength of the relationship between SST values

predicted by the model (HYCOM SST) and those from the climatology (Pathfinder SST). The latter is interpolated to the model grid for model–data comparisons. We evaluate time series of monthly mean SST at each model grid point over the Black Sea. Following Murphy (1988), the statistical relationships between the monthly mean Pathfinder SST (X) and HYCOM SST (Y) can be expressed as follows:

$$\mathrm{ME} = \overline{Y} - \overline{X}, \tag{1}$$

$$\mathrm{rms} = \left[\frac{1}{n}\sum_{i=1}^{n}(Y_i - X_i)^2\right]^{1/2}, \tag{2}$$

$$R = \frac{1}{n}\sum_{i=1}^{n}(X_i - \overline{X})(Y_i - \overline{Y})/(\sigma_X\sigma_Y), \tag{3}$$

$$\mathrm{SS} = R^2 - \underbrace{[R - (\sigma_Y/\sigma_X)]^2}_{B_{\mathrm{cond}}} - \underbrace{[(\overline{Y} - \overline{X})/\sigma_X]^2}_{B_{\mathrm{uncond}}}, \tag{4}$$

where $n = 12$, ME is the mean error, rms is the root-mean-square difference, R is the correlation coefficient, SS is the skill score, and $\overline{X}(\overline{Y})$and σ_X (σ_Y) are the mean and standard deviations of the Pathfinder (HYCOM) SST values, respectively.

The nondimensional SS in (4) includes conditional and unconditional biases (Murphy 1992). It is used for the model–data comparisons because one needs to examine more than the shape of the seasonal cycle using R. The nondimensional SS measures the accuracy of SST simulations relative to Pathfinder SST. The conditional bias (B_{cond}) is the bias in standard deviation of the HYCOM SST, while the unconditional bias (B_{uncond}) is the mismatch between the mean HYCOM and Pathfinder SST. The value of R^2 can be considered a measure of "potential" skill, that is, the skill that one can obtain by eliminating bias from the HYCOM SST. Note that the SS is 1.0 for perfect HYCOM SSTs, and positive SS is considered as a successful simulation. The nondimensional SS takes bias into account, something not done by R. Part of the reduction in SS values in comparison to R stems from the squaring of correlation in the SS calculation. Biases are taken into account in the rms differences, but in some cases the latter can be small when SS and R are poor. This can occur where the amplitude of seasonal cycle is small.

Annual mean HYCOM SST error and rms SST difference calculated over the seasonal cycle with respect to the Pathfinder climatology are shown in Fig. 9. The SST bias is small ($<0.25°$) in most of the Black Sea, and this is true regardless of the atmospheric forcing product used in the model simulations except for NCEP. This is clearly evident from the basin-averaged ME values (Table 6). There are relatively cold and warm SST biases in different regions of the Black Sea for NCEP forcing, but they tend to cancel in the areal average, resulting in small ME (Fig. 9a). For a given wind forcing, HYCOM usually gives slightly warm SST bias (i.e., ME $> 0°$C) in the interior of the Black Sea when using thermal forcing from EC10m. On the other hand, the reverse is true when using thermal forcing from NOGAPS. The most obvious feature of the ME maps is that HYCOM SST errors are relatively large (1°–2°C) near the coastal regions, especially on the northeastern coast near the Caucasus Peninsula (Fig. 1), in comparison to the interior of the region for all of the wind forcing products.

Some of the errors very close to the coastal regions (e.g., near Caucasus Peninsula) are primarily caused by the incorrect land–sea masks that exist in the atmospheric forcing products (Kara et al. 2005b). This results from problems representing sea points near land in the atmospheric forcing for the HYCOM simulations. In particular, a serious problem arises when using these coarse-resolution products (1.125° × 1.125° for EC10m and 1.875° × 1.875° for NCEP) in forcing fine-resolution (1/25° × 1/32°) Black Sea HYCOM. This is because atmospheric forcing values over water during interpolation to the finer ocean grid are contaminated by those over the land near the coastal regions mainly because of the much coarser atmospheric computational grid. A creeping sea-fill methodology could be a solution to reduce the improper representation of scalar atmospheric forcing parameters near coastal regions, although such methodology is only designed to apply thermal forcing parameters rather than vector fields, such as wind stress forcing (Kara et al. 2005, manuscript submitted to *J. Phys. Oceanogr.*).

A final remark about the ME maps is that the use of wind forcing from NCEP in the model simulations gives relatively large mean SST errors in comparison to those from other wind products. This is true when using thermal forcing from either EC10m or NOGAPS. In this case, HYCOM SST bias can be as large as 2°–3°C or even >3°C east of Trabzon (labeled on Fig. 1) in the easternmost part of the Black Sea. However, it should be emphasized that the atmospheric forcing from the operational model products is not quite correct in the easternmost part of the Black Sea. For example, examining the EC10m reanalysis product during 1979–93, Schrum et al. (2001) confirmed that the air temperature at 10 m above the sea surface is unrealistically low, and the air mixing ratio at 10 m above the sea surface is large in comparison to the climatic data from the observation-based climatologies in the easternmost region. Thus, some of the model errors in predicting the

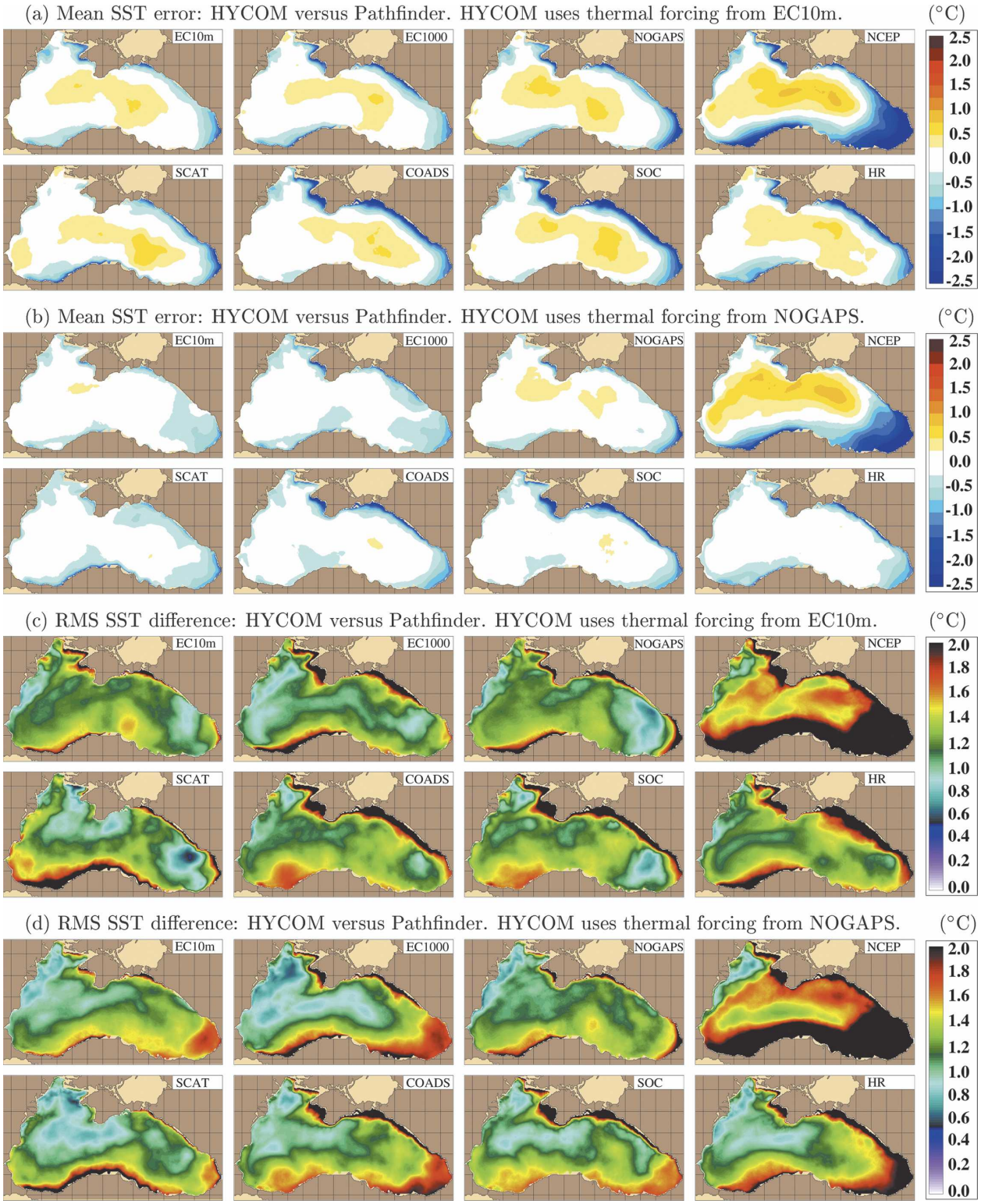

FIG. 9. Spatial mean error (ME) and rms difference maps between HYCOM SST and the Pathfinder SST climatology (HYCOM − Pathfinder) over the Black Sea. HYCOM was forced by eight different wind stress products using thermal forcing from (a) EC10m and (b) NOGAPS, separately. Note that all climatologically forced model simulations are performed without assimilation of any SST, and there is no relaxation to any SST climatology.

TABLE 6. Basin-averaged SST verification statistics: the 3.2-km HYCOM vs the 9.3-km Pathfinder climatology. The latter is interpolated onto the model grid for comparisons. Results are shown for the model response when forced with each individual wind product. Thermal forcing is from either EC10m or NOGAPS when using various wind forcing products. Statistics are calculated using monthly mean values (i.e., monthly mean HYCOM SST vs monthly mean Pathfinder SST) at each model grid point. An SS value of 1 indicates perfect HYCOM simulation with respect to the Pathfinder SST climatology. All R values are >0.97 and statistically significant in comparison to a 0.7 correlation value at a 95% confidence interval. A correlation coefficient of 0.98 is not statistically different from a correlation coefficient of 0.99.

	HYCOM uses thermal forcing from EC10m					
Wind forcing	ME (°C)	Rms (°C)	B_{cond}	B_{uncond}	SS	R
EC10m	0.00	1.24	0.02	0.00	0.96	0.99
EC1000	−0.04	1.27	0.03	0.00	0.95	0.99
NOGAPS	−0.01	1.25	0.02	0.00	0.96	0.99
NCEP	−0.40	2.26	0.09	0.01	0.86	0.98
SCAT	−0.01	1.29	0.03	0.00	0.95	0.99
COADS	−0.10	1.39	0.03	0.00	0.95	0.99
SOC	−0.10	1.38	0.03	0.01	0.95	0.99
HR	−0.06	1.45	0.02	0.00	0.94	0.98
	HYCOM uses thermal forcing from NOGAPS					
Wind forcing	ME (°C)	Rms (°C)	B_{cond}	B_{uncond}	SS	R
EC10m	−0.10	1.24	0.02	0.00	0.96	0.99
EC1000	−0.20	1.26	0.02	0.00	0.96	0.99
NOGAPS	−0.04	1.24	0.02	0.00	0.96	0.99
NCEP	−0.30	2.25	0.09	0.01	0.86	0.98
SCAT	−0.20	1.21	0.02	0.00	0.96	0.99
COADS	−0.30	1.35	0.03	0.00	0.95	0.99
SOC	−0.20	1.32	0.03	0.00	0.95	0.99
HR	−0.20	1.39	0.03	0.00	0.95	0.99

SST annual cycle can be attributed to the atmospheric forcing used in the simulations.

Similarly, wind speed from NCEP is much larger on basin average (>5 m s^{-1}) from Fig. 2a than from the other products mainly because it is so much stronger in the easternmost area. In fact, wind speeds from NCEP are usually at least twice as strong as from other atmospheric forcing products in the southeasternmost region of the Black Sea. This is an indication that such large wind speeds are unrealistic. The amplitude of the wind stress seasonal cycle based on the NCEP was also found to be unrealistically larger than the one estimated from the EC10m by Schrum et al. (2001), who used a different time period (1980–86) to construct the NCEP climatology. It is obvious that the wind forcing from NCEP is in error in the Black Sea, resulting in unrealistic model simulations.

Using an OGCM, Oguz and Malanotte-Rizzoli (1996) indicated that the monthly climatological surface fluxes impose too much cooling on the northwestern shelf during winter and too much warming in the eastern basin during summer, resulting in unrealistic SST simulations from their model. Such large biases do not exist in HYCOM simulations, partly explaining the importance of using 1) high-quality atmospheric forcing along with a hybrid coordinate model approach with no SST assimilation or relaxation, and 2) model SST in calculating latent and sensible heat fluxes rather than using net fluxes in model simulations. However, direct comparison between the two models is not the subject of this paper.

The rms SST differences between HYCOM and the Pathfinder climatology are generally small, typically about 1.2°C in the interior (Fig. 9b). This is true for all wind forcing products except NCEP with thermal forcing from EC10m and NOGAPS. The rms SST difference becomes large (>2°C) in the southern Black Sea when HYCOM is forced with NCEP winds along with thermal forcing from either EC10m or NOGAPS. In particular, the HYCOM simulation using NCEP winds resulted in the largest basin-averaged rms SST difference with a value of 2.16°C (2.15°C) when using thermal forcing from EC10m (NOGAPS) as seen from Table 6. The impact of using a fine-resolution wind forcing in the model simulations is most easily seen in the northwestern shelf, including the coastal regions near the Crimea Peninsula. In particular, the rms SST difference is reduced by 1° to 1.5°C when the model is forced with SCAT winds, which have a resolution of 0.25° × 0.25°. It should be emphasized that SCAT winds were produced from measurements that were all taken over the water, that is, there are no land values in the interpolated model forcing field. The rms SST difference is generally small (≈0.5°C) in the easternmost part of the Black Sea for a given wind forcing when using thermal forcing from EC10m (e.g., off Trabzon) as opposed to using thermal forcing from NOGAPS. On the contrary, the reverse is true in the interior, that is, the use of thermal forcing from NOGAPS tends to reduce rms SST difference. HYCOM is usually relatively insensitive to the thermal forcing in comparison to the wind forcing as evident from all rms SST difference maps, at least for the two forcing products (EC10m and NOGAPS) used in this paper.

HYCOM success in predicting SST is especially evident from the nondimensional SS values (>0.96) in almost all simulations over the majority of the Black Sea (Fig. 10a). Based on the SS definition (4), any positive SS value is considered as representative of a successful simulation, and all the HYCOM simulations yielded SS values much greater than zero. Even the HYCOM

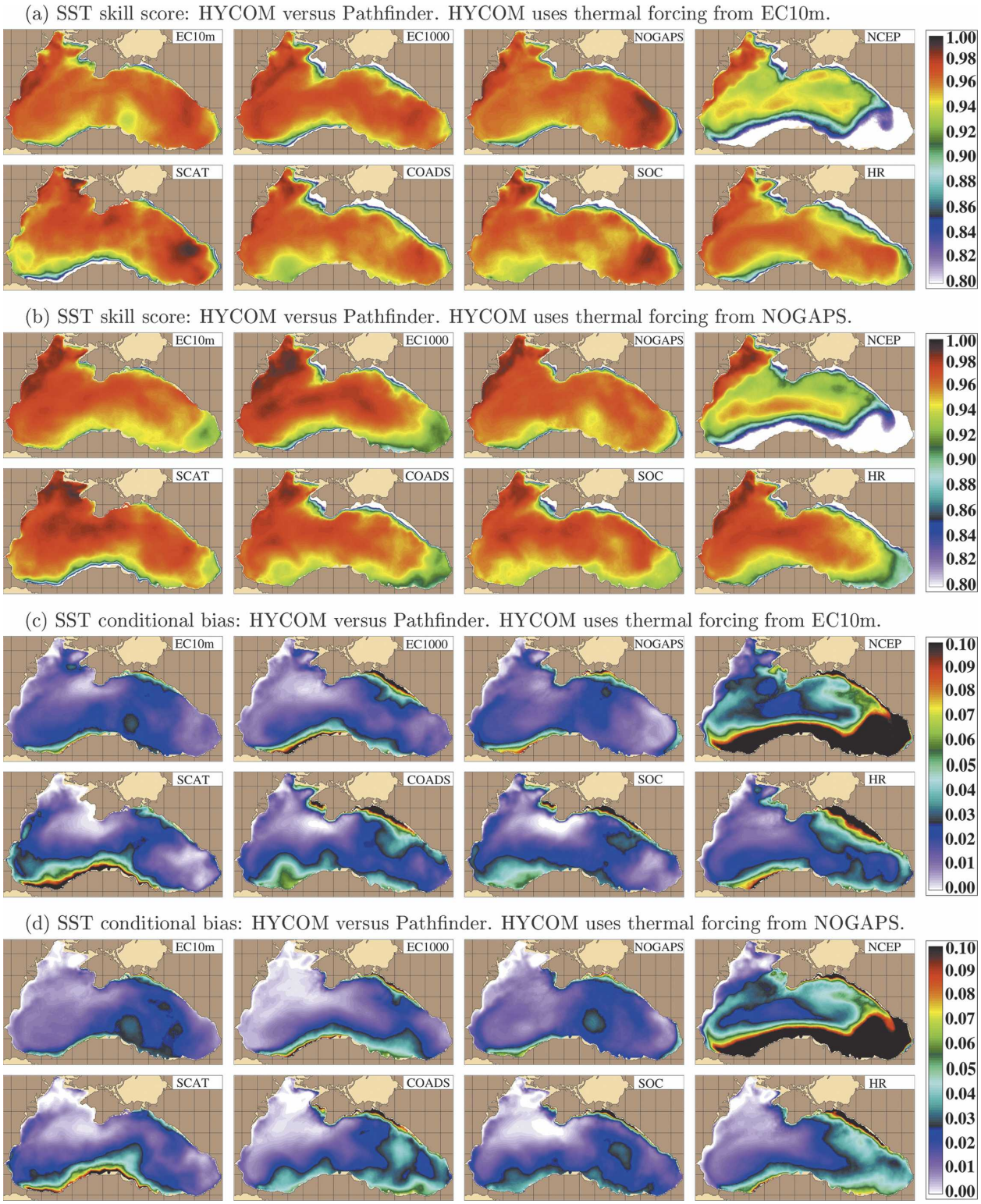

FIG. 10. Nondimensional SST skill score (SS) and SST conditional bias (B_{cond}) maps between HYCOM and the Pathfinder climatology over the Black Sea. HYCOM was forced by eight different wind stress products using thermal forcing from (a) EC10m and (b) NOGAPS, separately. In these comparisons the Pathfinder SST climatology is treated as "perfect." An SS value of 1.0 indicates perfect SST simulations from HYCOM. Note that all climatologically forced model simulations are performed with no assimilation of any SST, and there is no relaxation to any SST climatology.

simulation forced with NCEP winds gives SS values (>0.8) over the most of the Black Sea despite the lowest skill in comparison to other simulations in predicting the SST.

Here it is worthwhile to note that SST standard deviation over the seasonal cycle is generally >5°C over the Black Sea. The relatively low SS from the NCEP-forced simulations corresponds to relatively inaccurate HYCOM SSTs in the Black Sea region, but the NCEP SS is quite high compared to the SS from a variety of atmospheric forcings in some other regions of the global ocean. For example, in the equatorial Pacific warm pool, SST standard deviation is very small (e.g., ≈0.5°C), and rms SST differences can be quite low. However, it is usually difficult to obtain positive SST skill in this region when using atmospherically forced OGCMs (e.g., Kara et al. 2003). When the model was forced with SCAT winds along with thermal forcing from either EC10m or NOGAPS, the agreement between HYCOM and Pathfinder SST is quite remarkable, especially in the coastal regions of the northwestern shelf. The use of the fine-resolution wind forcing reduced rms SST differences in these regions (Fig. 9b).

It is noteworthy that the contributions to SS are from R^2, B_{cond}, and B_{uncond} as given in (4). Both biases are very small with values close to zero, and correlations are significantly large over the Black Sea (see Table 6). In particular, B_{cond} values are relatively larger than B_{uncond} regardless of the wind or thermal forcing used in the model simulations. This means that SST errors are due mostly to the bias in the standard deviation rather than bias in the mean. Spatial maps of B_{cond} are shown in Fig. 10b. Because B_{uncond} values are almost zero, and R values are very large (>0.98), their maps are not included here.

Major differences in all model simulations are seen in the coastal regions where, unlike SCAT, the coarse-resolution atmospheric forcing products were usually contaminated from land values. The SST simulations were improved when using SCAT winds, especially along the northwestern shelf where rms difference values were <0.5°C. It should be emphasized that the atmospheric forcing fields used in model simulations show considerable differences not simply due to native grid resolution or methodology for obtaining them, but may be partly due to the differences in averaging periods ranging from several years (i.e., SCAT and NOGAPS) to 100 yr (HR). For this reason, the focus in presenting model results was the HYCOM SST response to different atmospheric forcing products, not the accuracy of the atmospheric forcing products themselves.

b. Importance of high-frequency wind forcing

As explained in section 2c, the hybrid wind approach is used in all HYCOM simulations. A primary reason for using high-frequency (6 h) climatological forcing is to get time-varying wind speeds. A particular question arises here. What is the importance of using high-frequency winds in the model simulations?

One of the HYCOM simulations using thermal and high-frequency wind forcing from NOGAPS is repeated with the same thermal forcing but with the monthly mean wind forcing to investigate the importance of using hybrid winds. Both simulations were started from the same initial state. Model–data comparisons demonstrate that the annual mean HYCOM SST obtained using the monthly mean wind forcing is much less accurate in comparison to the Pathfinder SST (Fig. 11). The mean model SST generally has a warm bias in the case of monthly mean wind forcing. This is expected because the vertical mixing tends to be low, allowing excessive warming in a shallow mixed layer that is too shallow (not shown) because the variability in wind stress is too low. By including appropriate variability in wind stress, the HYCOM simulation using the high-frequency winds generates mixing, distributing heat over a thicker mixed layer and entraining more cold water from below (not shown), resulting in realistic SSTs. Thus, it is clear that a mixed layer model tuned with monthly winds cannot be optimal for interannual high-frequency forcing. Note that the 6-h submonthly wind stress anomalies in HYCOM have zero monthly mean wind stress, but they don't have a zero monthly mean wind speed. This implies that some of the SST improvement obtained from the high-frequency wind forcing may be due to improved average wind speed.

5. Sea surface circulation

Wind stress curl from the eight wind products is very different over the Black Sea (see section 2). Therefore, the main features of the climatological mean sea surface circulation simulated under different wind forcing is briefly investigated in this section. Thus, if results from this paper are used in selecting atmospheric forcing products, simulation of both the circulation and the mixed layer/SST can be considered.

The surface circulation system over the Black Sea has been investigated in various studies using observations, ocean models, and satellite images (e.g., Stanev 1990; Oguz et al. 1995; Stanev et al. 1997; Gawarkiewicz et al. 1999; Staneva et al. 2001; Afanasyev et al. 2002; Ginzburg et al. 2002; Korotaev et al. 2003; Zatsepin et al. 2003). These studies generally reveal the main point

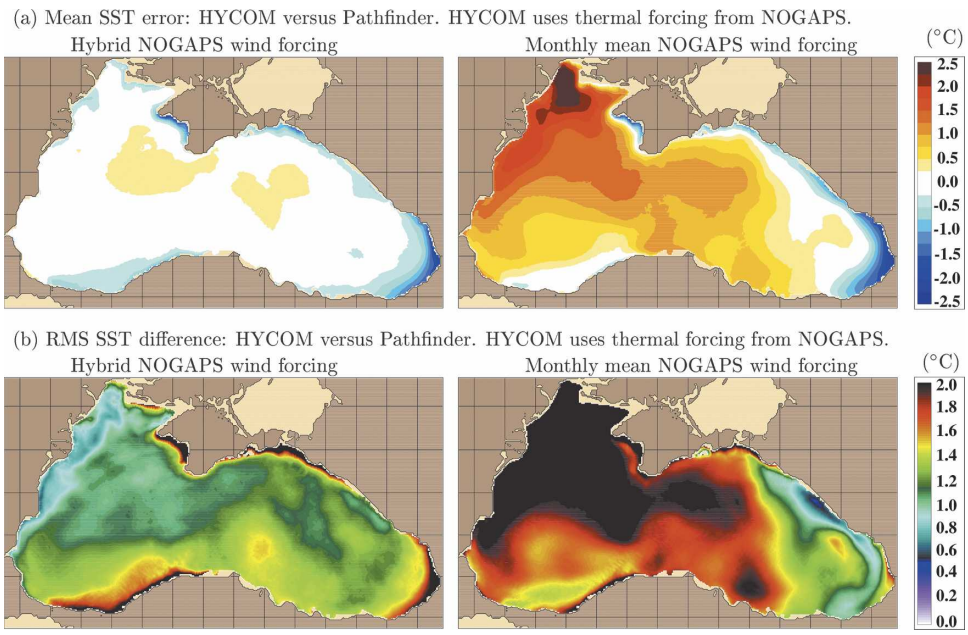

FIG. 11. Comparisons of climatologically forced HYCOM simulations using high-frequency vs monthly mean wind forcing: (a) annual mean model SST error and (b) rms SST difference. Both (a) and (b) are calculated with respect to the Pathfinder climatology. The basin-averaged annual mean SST biases are −0.04° and 1.79°C for the high-frequency and monthly wind forcing cases, respectively. Similarly, rms SST difference calculated over the seasonal cycle increases significantly from 1.24°C (high-frequency wind forcing) to 2.29°C (monthly mean wind forcing), demonstrating the impact of high-frequency wind forcing in the eddy-resolving OGCM simulations.

that the permanent feature of the upper-layer circulation is the Rim Current, which forms a cyclonic gyre around the entire continental shelf of the Black Sea, including two well-organized gyres in the interior. This cyclonic circulation is driven by the quasi-permanent positive wind stress curl field. Based on limited observations, the current speed, which varies seasonally, can be up to 40 cm s^{-1} or even higher along the Rim Current (Oguz et al. 1993).

The climatologically forced HYCOM simulations forced with eight wind stress products give very different spatial patterns for mean sea surface circulation (Fig. 12). The thermal forcing is from EC10m in all simulations. The velocity vectors from the 3.2-km HYCOM are subsampled to display the general surface circulation clearly. The western and eastern cyclonic gyres in the interior are well-known features of the Black Sea circulation, and they are reproduced when HYCOM uses wind forcing from EC10m and NOGAPS.

Korotaev et al. (2003) reports a current speed of 50 cm s^{-1} within the Rim Current near the sea surface with the use of data assimilation. Although there is no assimilation of any ocean data in our model simulations (except for relaxation to SSS), HYCOM forced with climatological wind stress products from EC10m, NOGAPS, and NCEP can give mean current speeds of >30 cm s^{-1}, even reaching maximum values of >45 cm s^{-1} (see arrow lengths in Fig. 12) near the western part of the Turkish coast as well. While the simulations performed with wind forcings from EC1000 and NCEP also demonstrate the existence of the Rim Current, they lack the closed cyclonic gyre systems in the interior. Observational-based climatologies, especially COADS and SOC, result in currents that are too weak, and the same is also partially true for SCAT.

Surface circulation features from HYCOM simulations using NOGAPS thermal forcing are found to be similar to those using EC10m thermal forcing (Fig. 12); therefore, they are not shown here. We only present the vector correlation between each simulation with EC10m thermal forcing and the corresponding simulation using NOGAPS thermal forcing for a given wind product. The vector correlation depends on the speed and the cosine of the angle between the two sets of vectors. Thus, vectors pointing in the same direction have a positive relationship and those pointing in opposite directions have a negative relationship (e.g., Crosby et al. 1993). The vector correlations are 0.99, 0.97, 0.98, and 0.99 when the wind forcing is from

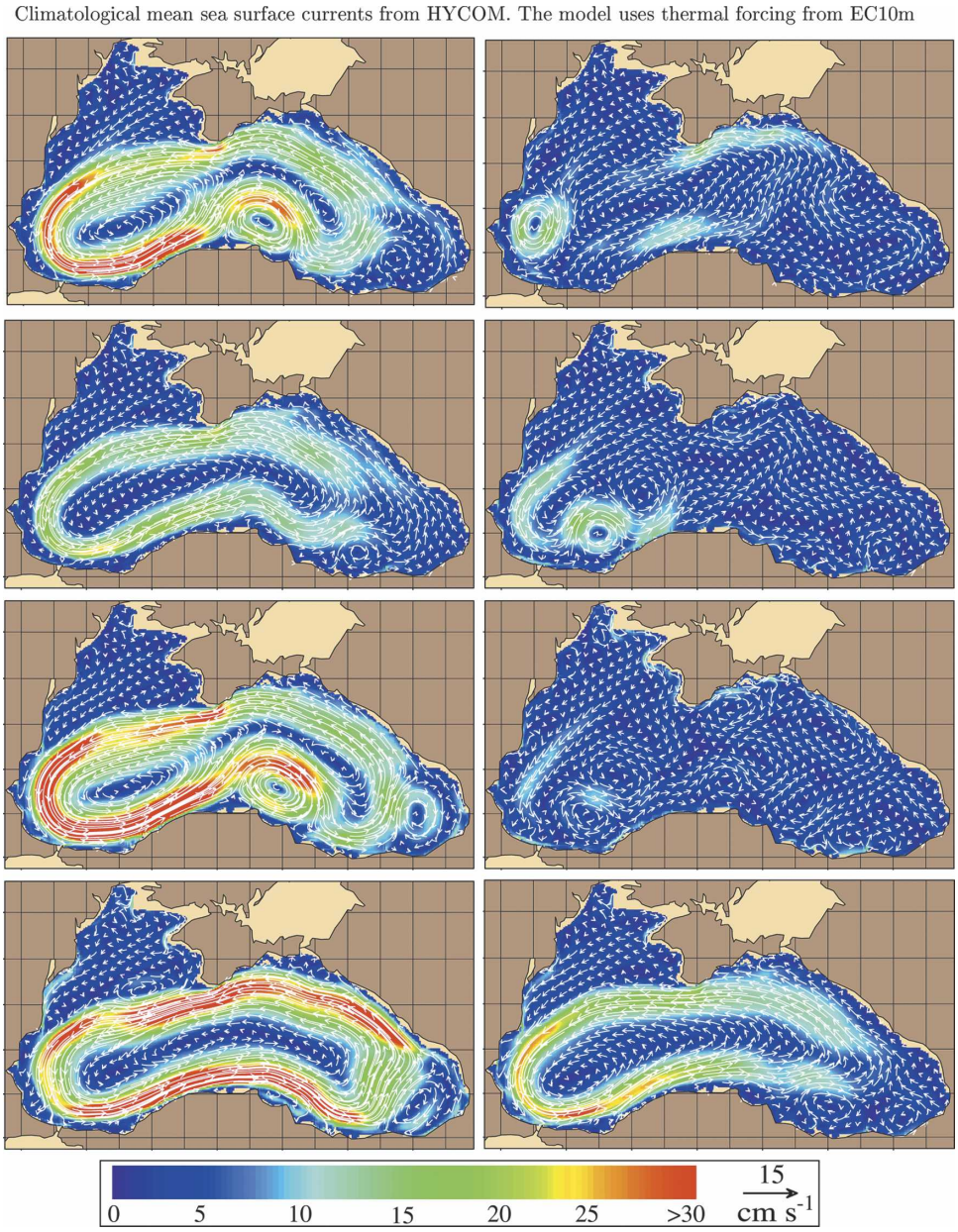

FIG. 12. Climatological mean sea surface currents overlaid on sea surface current speeds (cm s^{-1}) obtained from HYCOM simulations forced with eight different wind stress products over the Black Sea. The thermal forcing is from EC10m in all simulations. The length of the reference velocity vector is 15 cm s^{-1}. The velocity vectors are subsampled for plotting. See section 2d in the text for construction of the wind and thermal forcing fields.

EC10m, EC1000, NOGAPS, and NCEP for the EC10m thermal forcing versus NOGAPS thermal forcing simulations. Therefore, almost all of the variance existing in simulations with EC10m thermal forcing is also explained by simulations using NOGAPS thermal forcing. Smaller vector correlations of 0.92, 0.91, 0.89, and 0.94 are found for the SCAT, COADS, SOC, and HR simulations, but they are still statistically significant. Thus, we conclude that the use of different thermal forcing (i.e., EC10m versus NOGAPS) does not have significant impact on spatial variations of the speed and direction of sea surface currents. On the other hand, vector correlations between HYCOM simulations using various wind forcings for a given thermal forcing can be quite variable (Table 7). For example, a strong relationship exists between sea surface current from any pair of

TABLE 7. Vector correlations of climatological mean sea surface currents between the pairs of HYCOM simulations forced with various wind stress products. The thermal forcing is either from EC10m or NOGAPS for a given wind forcing set.

Wind forcing	HYCOM uses thermal forcing from EC10m							
	EC10m	EC1000	NOGAPS	NCEP	SCAT	COADS	SOC	HR
EC10m	1.00	0.82	0.92	0.75	0.35	0.45	0.26	0.79
EC1000	0.82	1.00	0.72	0.84	0.49	0.52	0.31	0.92
NOGAPS	0.92	0.72	1.00	0.75	0.31	0.45	0.27	0.76
NCEP	0.75	0.84	0.75	1.00	0.45	0.45	0.22	0.80
SCAT	0.35	0.49	0.31	0.45	1.00	0.24	0.09	0.39
COADS	0.45	0.52	0.45	0.45	0.24	1.00	0.68	0.53
SOC	0.26	0.31	0.27	0.22	0.09	0.68	1.00	0.34
HR	0.79	0.92	0.76	0.80	0.39	0.53	0.34	1.00
Wind forcing	HYCOM uses thermal forcing from NOGAPS							
	EC10m	EC1000	NOGAPS	NCEP	SCAT	COADS	SOC	HR
EC10m	1.00	0.74	0.96	0.76	0.41	0.34	0.25	0.71
EC1000	0.74	1.00	0.70	0.83	0.42	0.48	0.28	0.91
NOGAPS	0.96	0.70	1.00	0.76	0.35	0.36	0.27	0.69
NCEP	0.76	0.83	0.76	1.00	0.37	0.39	0.21	0.80
SCAT	0.41	0.42	0.35	0.37	1.00	0.07	0.04	0.38
COADS	0.34	0.48	0.36	0.39	0.07	1.00	0.76	0.48
SOC	0.25	0.28	0.27	0.21	0.04	0.76	1.00	0.32
HR	0.71	0.91	0.69	0.80	0.38	0.48	0.32	1.00

EC10m, EC1000, NOGAPS, NCEP, and HR, with the highest one between EC10m and NOGAPS, a value of 0.96 when thermal forcing from NOGAPS is used for both. With only one exception, all other pairings yield a lower vector correlation than the lowest between any of the preceding, with the lowest value being 0.04 between SCAT and SOC when NOGAPS thermal forcing is used. This quantitative evaluation and the earlier comparisons for the Rim Current indicate relative accuracy of sea surface currents from HYCOM simulations forced with EC10m, EC1000, NOGAPS, NCEP, and HR.

Sea surface circulation is also examined on the northwestern shelf (Fig. 13). This is the region where current speeds are relatively weak in comparison to those in most of Black Sea, including the main pathways of the Rim Current (Fig. 12). There are noticeable differences in the strength and structure of climatological mean sea surface currents on the shallow northwestern shelf. The model response to atmospheric wind forcing is quite effective on the locations of small eddies and gyres, while all simulations generally reveal the big gyre centered around 30°E except NCEP. The HR simulation also gives the basic features of the Rim Current even if its original spacing (2.0° × 2.0°) is very large for a small basin, such as Black Sea. In addition, relatively strong upwelling along the eastern boundary is a common feature of the model simulations.

HYCOM simulation forced with the SCAT winds reveals two eddies between 45°40′N and 46°N in the eastern part of the northwestern shelf (see Fig. 13) that are absent in all other simulations. The main shortcoming of the SCAT winds is the numerical noise at the scale of two grid intervals, which generates these oceanic eddies at the scales of 0.5° or so. Although the use of satellite-based SCAT wind stress resulted in very reliable SST simulations from HYCOM (see section 4), relatively poor simulation of sea surface circulation could be due to the short observational time period (August 1999 through March 2002) used for constructing the climatology over the Black Sea. SCAT also has an accuracy of 20° for wind direction (http://winds.jpl.nasa.gov/missions/quikscat/).

It is obvious that circulation features are quite similar and complex on the northwestern shelf even though the wind forcing is so poorly resolved, except SCAT. This indicates that in addition to wind stress, other constraints, such as bottom topography (1-min resolution used here), the coastline and riverline outflow strongly affects the surface circulation of the northwestern shelf, but such detailed investigation is beyond the focus of this paper.

6. Summary and conclusions

The development of a high-resolution ocean general circulation model (OGCM) of the Black Sea is a great challenge since there are not many eddy-resolving model studies in the region. Observations over the Black Sea are also too sparse and inhomogeneous to

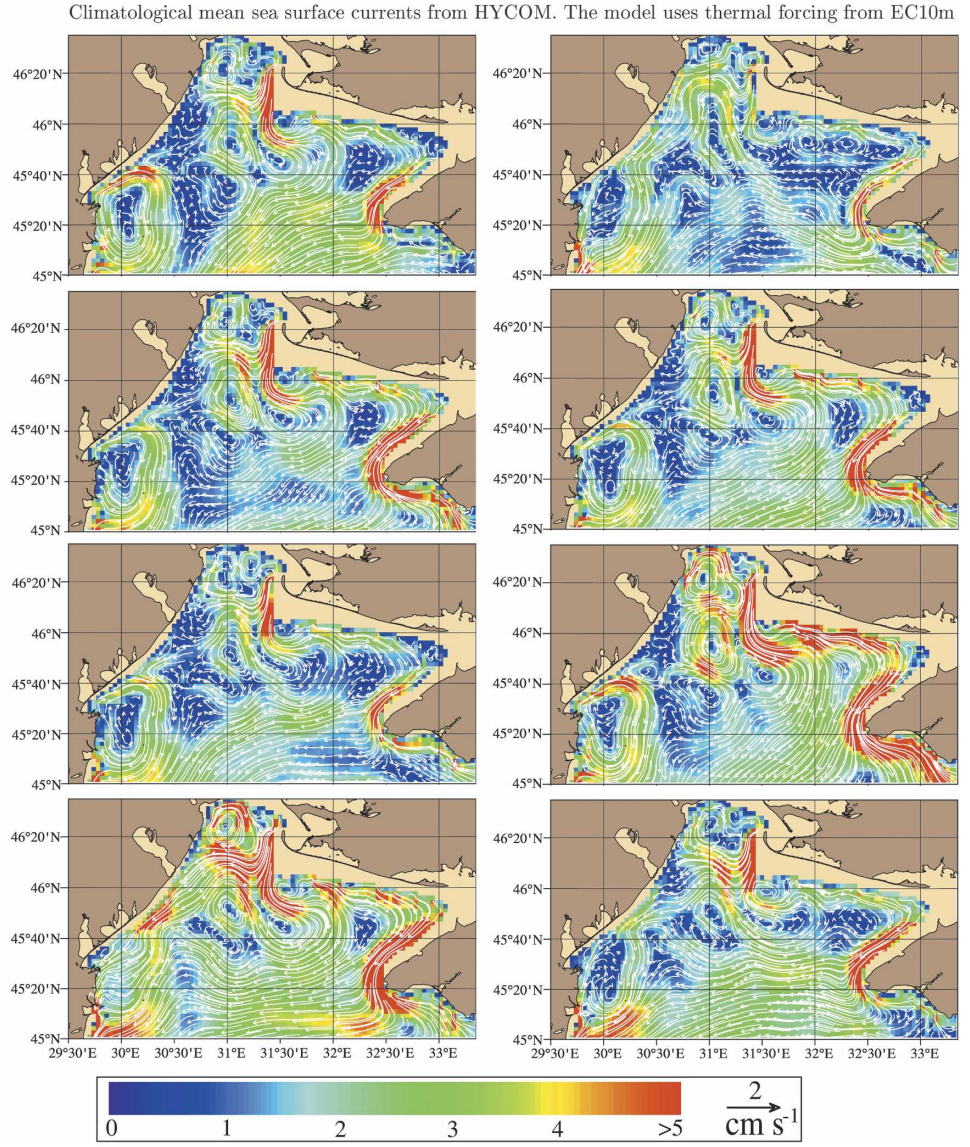

FIG. 13. Same as in Fig. 12, but for currents in a zoom region on a small part of the northwestern shelf where water depths are generally <60 m. Note that the length of the reference velocity vector is 2 cm s^{-1}, and mean current speeds are very weak. The velocity vectors are subsampled for plotting currents obtained from the eddy-resolving (≈3.2 km) HYCOM simulations.

produce the fine-resolution and high-quality climatologies that can be used as atmospheric forcing in OGCM studies. Therefore, wind stress and thermal forcing parameters presented in this paper are aimed at providing atmospheric forcing for OGCMs and other possible studies of the Black Sea. The sensitivity of climatologically forced simulations to these products is then examined using a fine-resolution (≈3.2 km) Hybrid Coordinate Ocean Model (HYCOM).

Eight wind forcing products were used to form atmospheric forcing parameters for the Black Sea. The three climatologies formed from the observation-based products are COADS, SOC. and HR; the four formed from operational model products are EC10m, EC1000, NOGAPS, and NCEP. Measurements from the Sea Winds scatterometer on the QuikSCAT satellite were also used to produce the finest-resolution (0.25° × 0.25°) climatological product (SCAT) for the Black Sea. Atmospheric forcing parameters were constructed under two categories: 1) wind forcing (wind stress) and 2) thermal forcing (air temperature and air mixing ratio at 10 m above the sea surface, precipitation, net shortwave radiation at the sea surface, and net solar radiation, which is the sum of net shortwave radiation and

net longwave radiation at the sea surface). Thermal forcing from EC10m or NOGAPS was used in all simulations.

It is demonstrated that some of the climatological forcing parameters reported in earlier studies, which are based on sparse local observations, include some errors. Previous observational and OGCM studies usually used or reported relatively large wind stresses as the wind speeds are larger than those reported in this study. Here, both observation-based climatologies and climatologies based on operational model products are shown to give a basin-averaged wind speed of 3–4 m s^{-1} in the Black Sea with the exception of the extreme value of 4.6 m s^{-1} from NCEP. Overall, observation-based climatologies (COADS, SOC, and HR) are too smooth. Consequently, they should not be used in eddy-resolving OGCM studies of the Black Sea or for similar smaller ocean basins. Basin-averaged annual mean values from EC10m and NOGAPS suggest very close estimates for evaporation and precipitation ($\approx$270 km^3 yr^{-1} for evaporation and $\approx$220 km^3 yr^{-1} for precipitation) in the Black Sea. These values are significantly lower than those reported in earlier studies ($\approx$350 km^3 yr^{-1} for evaporation and $\approx$ 300 km^3 yr^{-1} for precipitation). Air temperatures at 10 m above the sea surface from EC10m and NOGAPS usually agree with those from local data sources except that operational models are 2°C colder from January through April.

Using eight wind products and two thermal forcing products (EC10m and NOGAPS), a total of 16 climatologically forced HYCOM simulations with no ocean data assimilation or SST relaxation (except for relaxation to climatological sea surface salinity) were performed to investigate the sensitivity of Black Sea HYCOM to the choice of atmospheric forcing product. Comparisons of monthly mean SST between HYCOM and a satellite-based climatology (Pathfinder) revealed that the best SST simulation was obtained when HYCOM used wind forcing from SCAT and thermal forcing from NOGAPS, with a basin-averaged rms difference value of 1.21°C and a skill score of 0.96 over the annual cycle. In particular, when HYCOM used thermal forcing from EC10m, basin-averaged rms SST differences with respect to the Pathfinder SST climatology are 1.24°, 1.27°, 1.25°, and 2.16°C when using wind forcing from EC10m, EC1000, NOGAPS, and NCEP (operational model products), respectively, and 1.39°, 1.38°, and 1.45°C when using wind forcing from COADS, SOC, and HR (observation-based products). These results remained nearly the same when HYCOM used thermal forcing from NOGAPS. Although net shortwave radiation from NOGAPS is larger than that from EC10m by $\approx$30 W m^{-2}, the use of these two products in the model simulations yielded similar SST results on climatological time scales. The simulated SSTs from all simulations are typically accurate to within $\approx$0.1° to $\approx$ 0.3°C in the interior of the Black Sea, when there is no assimilation of SST data and when the model SST is used in calculation of latent and sensible heat fluxes. The paper also demonstrates that the model skill in simulating the annual SST cycle improves significantly when using high-frequency wind forcing, which is composed of 6-h wind stress anomalies added to the monthly mean wind stress.

While the model SST response to the various atmospheric forcing products usually remained robust in the HYCOM simulations, the wind stress patterns and magnitudes from the eight atmospheric forcing products presented in this paper clearly imply that the choice of the atmospheric forcing product can have large influences on the simulated sea surface circulation features of the Black Sea. The location and strength of the Rim Current vary greatly, depending on the atmospheric wind product used. Although the use of SCAT wind improves the accuracy SST simulations because of its fine resolution and accuracy near coastal regions, it does not provide very realistic circulation features. Thus, the best atmospheric forcing for simulating SST is not necessarily the best for simulating Black Sea circulation because of relative sensitivity to wind speed and wind stress curl.

HYCOM simulations forced with observation-based wind stress climatologies (e.g., COADS and SOC) yield weak surface current speeds and disorganized Rim Current structure over the continental shelf. Additionally, the locations of small gyres and eddies remain almost robust regardless of the wind forcing product used in HYCOM simulations over the northwestern shelf. This suggests that other constraints, such as the topography, coastline, and riverline inflow, have a larger impact than atmospheric forcing on the sea surface circulation in this region.

Given that HYCOM SST simulations are relatively poor near coastal regions, there is a clear message for regional and coastal ocean modelers. There are systematic biases in gridded atmospheric forcing products (such as EC10m, NOGAPS, and NCEP) near coastal boundaries when the spatial resolution is too poor to sample these regions appropriately, that is, at the scale of a much finer ocean grid (e.g., 3.2-km HYCOM). For many studies in which an accurate representation of the ocean dynamics and atmospheric forcing is needed close to the coastline, a procedure is needed to reduce land contamination. The availability of satellite-derived atmospheric forcing products (e.g., SCAT winds) with a higher spatial resolution than weather center analyses is

very promising for future studies focused mainly on atmospheric forcing near land–sea boundaries. Another valuable step would be atmospheric forcing products from weather centers that are provided on their computational model grid for use in fine-resolution OGCM studies, especially in coastal regions.

Finally, this paper utilizes a single ocean model design (HYCOM) in examining the impact of atmospheric forcing on the SST simulations. While worthwhile and interesting, including additional Black Sea model designs is beyond the scope of this paper but is a worthwhile topic for future research. Investigating the seasonal variability of various atmospheric forcing products, such as those discussed here, is another subject for future study.

Acknowledgments. The numerical HYCOM simulations were performed under the Department of Defense High Performance Computing Modernization Program on an IBM SP POWER3 at the Naval Oceanographic Office, Stennis Space Center, Mississippi, and on a HP/COMPAQ SC45 at the United States Army Engineer Research and Development Center (ERDC), Vicksburg, Mississippi. We thank G. Halliwell of University of Miami and E. J. Metzger and J. F. Shriver of the Naval Research Laboratory (NRL) for their discussions. The authors would also like to acknowledge two reviewers, T. Oguz and E. V. Stanev, who provided helpful suggestions. This research is funded by the Office of Naval Research (ONR) under Program Element 601153N as part of the NRL 6.1 Dynamics of Low Latitude Western Boundary Current (DLLWBC) project. This is paper has been approved for public release by the Naval Research Laboratory.

REFERENCES

Afanasyev, Y. D., A. G. Kostianoy, A. G. Zatsepin, and P.-M. Poulain, 2002: Analysis of velocity field in the eastern Black Sea from satellite data during the Black Sea '99 experiment. *J. Geophys. Res.,* **107,** 3098, doi:10.1029/2000JC000578.

Altman, E. N., and N. I. Kumish, 1986: Interannual and seasonal variability of the Black Sea fresh water balance (in Russian). *Tr. Gos. Okeanogr. Inst.,* **145,** 3–15.

——, I. F. Gertman, and Z. A. Golubeva, 1987: Climatological fields of salinity and temperature in the Black Sea (in Russian). State Oceanography Institute Tech. Rep., 109 pp. [Available from the State Oceanography Institute, Sevastopol Branch, Sevastopol, Ukraine.]

Bleck, R., 2002: An oceanic general circulation model framed in hybrid isopycnic-Cartesian coordinates. *Ocean Modell.,* **4,** 55–88.

Bourassa, M. A., D. M. Legler, J. J. O'Brien, and S. R. Smith, 2003: SeaWinds validation with research vessels. *J. Geophys. Res.,* **108,** 3019, doi:10.1029/2001JC001028.

——, R. Rosario, S. R. Smith, and J. J. O'Brien, 2005: A new FSU winds climatology. *J. Climate,* **18,** 3692–3704.

Bourras, D., L. Eymard, and W. T. Liu, 2002: A neural network to estimate the latent heat flux over oceans from satellite observations. *Int. J. Remote Sens.,* **23,** 2405–2423.

Casey, K. S., and P. Cornillon, 1999: A comparison of satellite and in situ–based sea surface temperature climatologies. *J. Climate,* **12,** 1848–1863.

Chassignet, E. P., L. T. Smith, G. R. Halliwell Jr., and R. Bleck, 2003: North Atlantic simulations with the Hybrid Coordinate Ocean Model (HYCOM): Impact of the vertical coordinate choice, reference pressure, and thermobaricity. *J. Phys. Oceanogr.,* **33,** 2504–2526.

Chelton, D. B., J. C. Ries, B. J. Haines, L. L. Fu, and P. Callahan, 2001: Satellite altimetry. *Satellite Altimetry and Earth Sciences,* L. L. Fu and A. Cazanave, Eds., Academic Press, 57–64.

Crosby, D. S., L. C. Breaker, and W. H. Gemmill, 1993: A proposed definition for vector correlation in geophysics: Theory and application. *J. Atmos. Oceanic Technol.,* **10,** 355–367.

da Silva, A. M., C. C. Young, and S. Levitus, 1994: *Algorithms and Procedures.* Vol. 1, *Atlas of Surface Marine Data 1994,* NOAA Atlas NESDIS 6, 83 pp.

Efimov, E. V., and A. Timofeev, 1990: Investigation of the Black Sea and Azov Sea heat balance. Ukrainian Academy of Science, Sevastopol, Ukraine, 237 pp.

Ezer, T., 1999: Decadal variabilities of the upper layers of the subtropical North Atlantic: An ocean model study. *J. Phys. Oceanogr.,* **29,** 3111–3124.

Fairall, C. W., E. F. Bradley, J. E. Hare, A. A. Grachev, and J. B. Edson, 2003: Bulk parameterization of air–sea fluxes: Updates and verification for the COARE algorithm. *J. Climate,* **16,** 571–591.

Fox, D. N., W. J. Teague, C. N. Barron, M. R. Carnes, and C. M. Lee, 2002: The Modular Ocean Data Assimilation System (MODAS). *J. Atmos. Oceanic Technol.,* **19,** 240–252.

Fu, L. L., and Y. Chao, 1997: The sensitivity of a global ocean model to wind forcing: A test using sea level and wind observations from satellites and operational wind analysis. *Geophys. Res. Lett.,* **24,** 1783–1786.

Gawarkiewicz, G., G. Korotaev, S. Stanichny, L. Repetin, and D. Soloviev, 1999: Synoptic upwelling and cross-shelf transport processes along the Crimean coast of the Black Sea. *Cont. Shelf Res.,* **19,** 977–1005.

Gibson, J. K., P. Kållberg, S. Uppala, A. Hernandez, A. Nomura, and E. Serrano, 1999: ECMWF Re-Analysis Project Report Series: 1. ERA description (Version 2), 74 pp. [Available from ECMWF, Shinfield Park, Reading RG2 9AX, United Kingdom.]

Ginzburg, A. I., A. G. Kostianoy, N. P. Nezlin, D. M. Soloviev, and S. V. Stanichny, 2002: Anticyclonic eddies in the northwestern Black Sea. *J. Mar. Syst.,* **32,** 91–106.

Gleckler, P. J., and B. C. Weare, 1997: Uncertainties in global ocean surface heat flux climatologies derived from ship observations. *J. Climate,* **10,** 2764–2781.

Golubev, Y. N., and A. Y. Kuftarkov, 1993: On the flux of momentum at the Black Sea surface (in Russian). *Meteor. Gidrol.,* **3,** 92–97.

Golubeva, A., 1984: Variability of the Black Sea heat balance (in Russian). *Tr. Gos. Okeanogr. Inst.,* **180,** 21–32.

Halliwell, G. R., Jr., 2004: Evaluation of vertical coordinate and vertical mixing algorithms in the HYbrid Coordinate Ocean Model (HYCOM). *Ocean Modell.,* **7,** 285–322.

Harrison, D. E., 1989: On climatological monthly mean wind stress and wind stress curl fields over the World Ocean. *J. Climate,* **2,** 57–70.

Hellerman, S., and M. Rosenstein, 1983: Normal monthly wind stress over the world ocean with error estimates. *J. Phys. Oceanogr.,* **13,** 1093–1104.

Hogan, P. J., and H. E. Hurlburt, 2005: Sensitivity of simulated circulation dynamics to the choice of surface wind forcing in the Japan/East Sea. *Deep-Sea Res.,* **52,** 1464–1489.

Jo, Y.-H., X.-H. Yan, J. Pan, and W. T. Liu, 2004: Sensible and latent heat flux in the tropical Pacific from satellite multisensor data. *Remote Sens. Environ.,* **90,** 166–177.

Josey, S. A., E. C. Kent, and P. K. Taylor, 1999: New insights into the ocean heat budget closure problem from analysis of the SOC air–sea flux climatology. *J. Climate,* **12,** 2856–2880.

——, ——, and ——, 2002: Wind stress forcing of the ocean in the SOC climatology: Comparisons with the NCEP–NCAR, ECMWF, UWM/COADS, and Hellerman and Rosenstein datasets. *J. Phys. Oceanogr.,* **32,** 1993–2019.

Kalnay, E., and Coauthors, 1996: The NCEP/NCAR 40-Year Reanalysis Project. *Bull. Amer. Meteor. Soc.,* **77,** 437–471.

Kara, A. B., H. E. Hurlburt, and P. A. Rochford, 2000: Efficient and accurate bulk parameterizations of air–sea fluxes for use in general circulation models. *J. Atmos. Oceanic Technol.,* **17,** 1421–1438.

——, ——, and ——, 2002: Air–sea flux estimates and the 1997–1998 ENSO event. *Bound.-Layer Meteor.,* **103,** 439–458.

——, A. J. Wallcraft, and H. E. Hurlburt, 2003: Climatological SST and MLD simulations from NLOM with an embedded mixed layer. *J. Atmos. Oceanic Technol.,* **20,** 1616–1632.

——, H. E. Hurlburt, P. A. Rochford, and J. J. O'Brien, 2004: The impact of water turbidity on the interannual sea surface temperature simulations in a layered global ocean model. *J. Phys. Oceanogr.,* **34,** 345–359.

——, A. J. Wallcraft, and H. E. Hurlburt, 2005a: A new solar radiation penetration scheme for use in ocean mixed layer studies: An application to the Black Sea using a fine-resolution Hybrid Coordinate Ocean Model (HYCOM). *J. Phys. Oceanogr.,* **35,** 13–32.

——, ——, and ——, 2005b: Sea surface temperature sensitivity to water turbidity from simulations of the turbid Black Sea using HYCOM. *J. Phys. Oceanogr.,* **35,** 33–54.

——, ——, and ——, 2005c: How does solar attenuation depth affect the ocean mixed layer? Water turbidity and atmospheric forcing impacts on the simulation of seasonal mixed layer variability in the turbid Black Sea. *J. Climate,* **18,** 389–409.

Kelly, K. A., S. Dickinson, and Z.-J. Yu, 1999: NSCAT tropical wind stress maps: Implications for improving ocean modeling. *J. Geophys. Res.,* **104,** 291–310.

Kent, E. C., and P. K. Taylor, 1995: A comparison of heat flux estimates for the North Atlantic Ocean. *J. Phys. Oceanogr.,* **25,** 1530–1549.

——, ——, B. S. Truscott, and J. A. Hopkins, 1993: The accuracy of voluntary observing ships' meteorological observations—Results of the VSOP-NA. *J. Atmos. Oceanic Technol.,* **10,** 591–608.

Korotaev, G. K., T. Oguz, A. Nikiforov, and C. J. Koblinsky, 2003: Seasonal, interannual and mesoscale variability of the Black Sea upper layer circulation derived from altimeter data. *J. Geophys. Res.,* **108,** 3122, doi:10.1029/2002JC001508.

Lee, S.-K., D. B. Enfield, and C. Wang, 2005: Ocean general circulation model sensitivity experiments on the annual cycle of the Western Hemisphere Warm Pool. *J. Geophys. Res.,* **110,** C09004, doi:10.1029/2004JC002640.

Liu, W. T., 2002: Progress in scatterometer application. *J. Oceanogr.,* **58,** 121–136.

——, W. Tang, and P. S. Polito, 1998: NASA Scatterometer provides global ocean-surface wind fields with more structures than numerical weather prediction. *Geophys. Res. Lett.,* **25,** 761–764.

Makerov, Y. V., 1961: Heat balance of the Black Sea (in Russian). *Tr. Gos. Okeanogr. Inst.,* **61,** 169–183.

Metzger, E. J., 2003: Upper ocean sensitivity to wind forcing in the South China Sea. *J. Oceanogr.,* **59,** 783–798.

Murphy, A. H., 1988: Skill scores based on the mean square error and their relationships to the correlation coefficient. *Mon. Wea. Rev.,* **116,** 2417–2424.

——, 1992: Climatology, persistence, and their linear combination as standards of reference in skill scores. *Wea. Forecasting,* **7,** 692–698.

Oguz, T., and P. Malanotte-Rizzoli, 1996: Seasonal variability of wind and thermohaline driven circulation in the Black Sea: Modeling studies. *J. Geophys. Res.,* **101,** 16 551–16 569.

——, ——, and D. Aubrey, 1995: Wind and thermohaline circulation of the Black Sea driven by yearly mean climatological forcing. *J. Geophys. Res.,* **100,** 6845–6863.

Pegion, P. J., M. A. Bourassa, D. M. Legler, and J. J. O'Brien, 2000: Objectively derived daily "winds" from satellite scatterometer data. *Mon. Wea. Rev.,* **128,** 3150–3168.

Perry, G. D., P. B. Duffy, and N. L. Miller, 1996: An extended data set of river discharges for validation of general circulation models. *J. Geophys. Res.,* **101,** 21 339–21 349.

Rachev, N. H., V. M. Roussenov, and E. V. Stanev, 1991: The Black Sea climatological wind stress (in Bulgarian). *Bulg. J. Meteor. Hydrol.,* **2,** 72–79.

Rienecker, M. M., R. Atlas, S. D. Schubert, and C. S. Willett, 1996: A comparison of surface wind products over the North Pacific Ocean. *J. Geophys. Res.,* **101,** 1011–1023.

Rosmond, T. E., J. Teixeira, M. Peng, T. F. Hogan, and R. Pauley, 2002: Navy Operational Global Atmospheric Prediction System (NOGAPS): Forcing for ocean models. *Oceanography,* **15,** 99–108.

Samuel, S. L., K. Haines, S. A. Josey, and P. G. Myers, 1999: Response of the Mediterranean Sea thermohaline circulation to observed changes in the winter wind stress field in the period 1980–93. *J. Geophys. Res.,* **104,** 7771–7784.

Schlax, M. G., D. B. Chelton, and M. H. Freilich, 2001: Sampling errors in wind fields constructed from single and tandem scatterometer datasets. *J. Atmos. Oceanic Technol.,* **18,** 1014–1036.

Schopf, P. S., and A. Loughe, 1995: A reduced-gravity isopycnal ocean model: Hindcasts of El Niño. *Mon. Wea. Rev.,* **123,** 2839–2863.

Schrum, C., J. Staneva, E. Stanev, and E. Ozsoy, 2001: Air–sea exchange in the Black Sea estimated from atmospheric analysis for the period 1979–1993. *J. Mar. Syst.,* **31,** 3–19.

Simonov, A. I., and E. N. Altman, 1991: *Black Sea.* Vol. 4, *Hydrometerology and Hydrochemistry of the USSR Seas,* Gidrometeoizdat, 430 pp.

Smith, S. R., D. M. Legler, and K. V. Verzone, 2001: Quantifying uncertainties in NCEP reanalyses using high-quality research vessel observations. *J. Climate,* **14,** 4062–4072.

Sorkina, A. I., 1974: *Reference Book on the Black Sea Climate* (in Russian). Gidrometeoizdat, 406 pp.

Stanev, E. V., 1990: On the mechanisms of the Black Sea circulation. *Earth-Sci. Rev.,* **28,** 285–319.

——, and J.-M. Beckers, 1999: Numerical simulations of seasonal and interannual variability of the Black Sea thermohaline circulation. *J. Mar. Syst.,* **22,** 241–267.

——, J. V. Staneva, and V. M. Roussenov, 1997: On the Black Sea water mass formation. Model sensitivity study to atmospheric forcing and parameterization of some physical processes. *J. Mar. Syst.,* **13,** 245–272.

——, M. J. Bowman, E. L. Peneva, and J. V. Staneva, 2003: Control of Black Sea intermediate water mass formation by dynamics and topography: Comparison of numerical simulations, survey and satellite data. *J. Mar. Res.,* **61,** 59–99.

——, J. Staneva, J. L. Bullister, and J. W. Murray, 2004: Ventilation of the Black Sea pycnocline. Parameterization of convection, numerical simulations and validations against observed chlorofluorocarbon data. *Deep-Sea Res.,* **51,** 2137–2169.

Staneva, J. V., and E. V. Stanev, 1998: Oceanic response to atmospheric forcing derived from different climatic data sets. *Ocean. Acta,* **21,** 393–417.

——, D. E. Dietrich, E. V. Stanev, and M. J. Bowman, 2001: Rim Current and coastal eddy mechanisms in an eddy-resolving Black Sea general circulation. *J. Mar. Syst.,* **31,** 137–157.

Sui, C.-H., X. Li, M. M. Rienecker, K.-M. Lau, and R. T. Pinker, 2003: The role of daily surface forcing in the upper ocean over the tropical Pacific: A numerical study. *J. Climate,* **16,** 756–766.

Townsend, T. L., H. E. Hurlburt, and P. J. Hogan, 2000: Modeled Sverdrup flow in the North Atlantic from 11 different wind stress climatologies. *Dyn. Atmos. Oceans,* **32,** 373–417.

Trenberth, K. E., and C. J. Guillemot, 1998: Evaluation of the atmospheric moisture and hydrological cycle in the NCEP/NCAR reanalyses. *Climate Dyn.,* **14,** 213–231.

——, D. P. Stepaniak, J. W. Hurrell, and M. Fiorino, 2001: Quality of reanalyses in the Tropics. *J. Climate,* **14,** 1499–1510.

Trukhchev, D. I., and Y. L. Demin, 1992: The Black Sea general circulation and climatic temperature and salinity fields. Woods Hole Oceanographic Institution Tech. Rep. WHOI-92-34, 136 pp. [Available from MBL/WHOI Library, 7 MBL Street, Woods Hole, MA 02543.]

Unluata, U., T. Oguz, M. A. Latif, and E. Ozsoy, 1990: On the physical oceanography of the Turkish Straits. *The Physical Oceanography of Sea Straits,* G. Pratt, Ed., NATO ASI Series C, Kluwer, 25–60.

Vörösmarty, C. J., K. Sharma, B. M. Fekete, A. H. Copeland, J. Holden, J. Marble, and J. A. Lough, 1997: The storage and aging of continental runoff in large reservoir systems of the world. *Ambio,* **26,** 210–219.

Wallcraft, A. J., A. B. Kara, H. E. Hurlburt, and P. A. Rochford, 2003: The NRL Layered Global Ocean Model (NLOM) with an embedded mixed layer submodel: Formulation and tuning. *J. Atmos. Oceanic Technol.,* **20,** 1601–1615.

Weare, B. C., 1989: Uncertainties in estimates of surface heat fluxes derived from marine reports over the tropical and subtropical oceans. *Tellus,* **41A,** 357–370.

Zatsepin, A. G., A. I. Ginzburg, A. G. Kostianoy, V. V. Kremenitskiy, V. G. Krivosheya, S. V. Stanichny, and P.-M. Poulain, 2003: Observations of Black Sea mesoscale eddies and associated horizontal mixing. *J. Geophys. Res.,* **108,** 3246, doi:10.1029/2002JC001390.

CORRIGENDUM

Due to a press error, Figs. 12 and 13 in "Black Sea Mixed Layer Sensitivity to Various Wind and Thermal Forcing Products on Climatological Time Scales," by A. Birol Kara, Harley E. Hurlburt, Alan J. Wallcraft, and Mark A. Bourassa, which was published in the *Journal of Climate,* Vol. 18, No. 24, 5266–5293, were missing labels on the figure panels. These figures are reproduced below in their entirety, as they were intended to be published.

The staff of the *Journal of Climate* regrets any inconvenience this error may have caused.

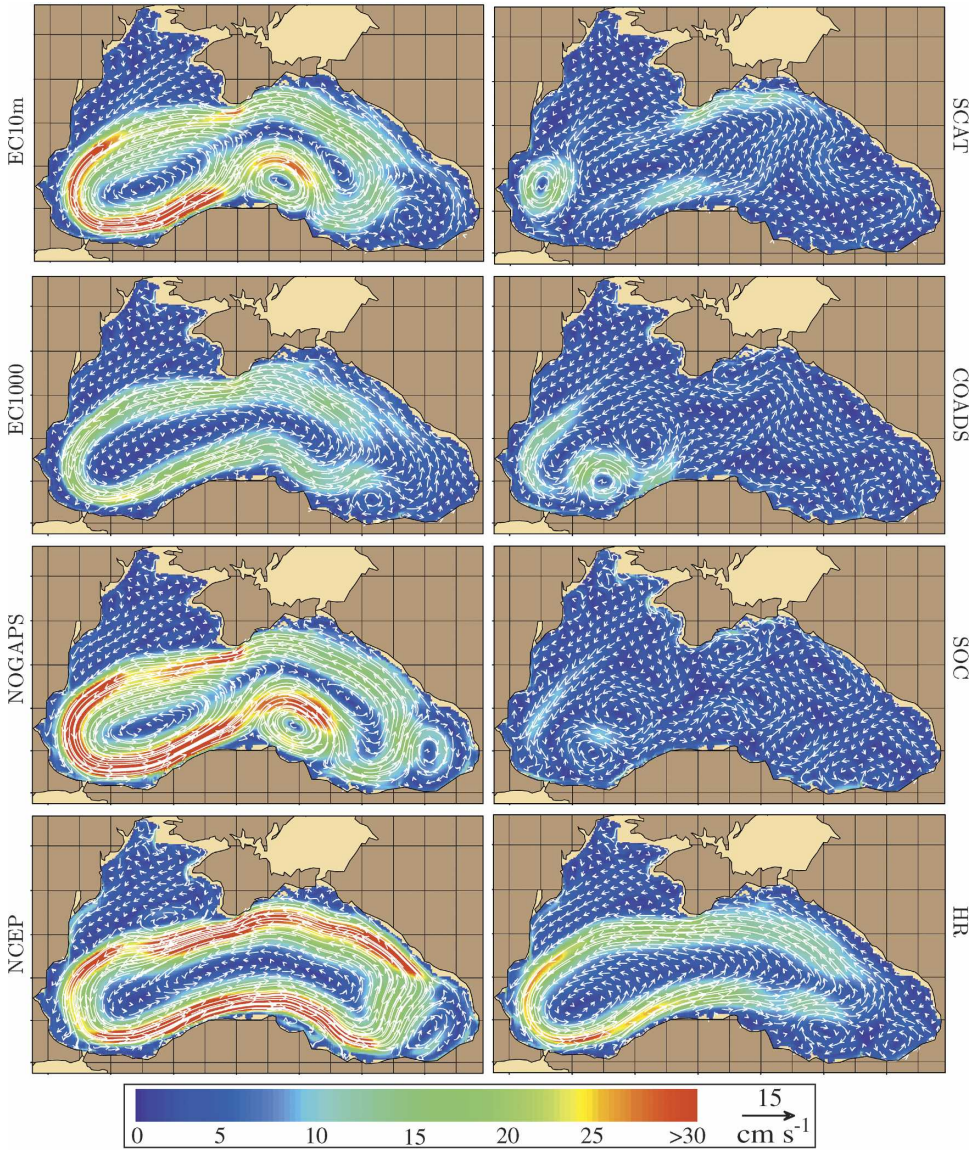

FIG. 12. Climatological mean sea surface currents over laid on sea surface current speeds (cm s^{-1}) obtained from HYCOM simulations forced with eight different wind stress products over the Black Sea. The thermal forcing is from EC10m in all simulations. The length of the reference velocity vector is 15 cm s^{-1}. The velocity vectors are subsampled for plotting. See section 2d in the text for construction of the wind and thermal forcing fields.

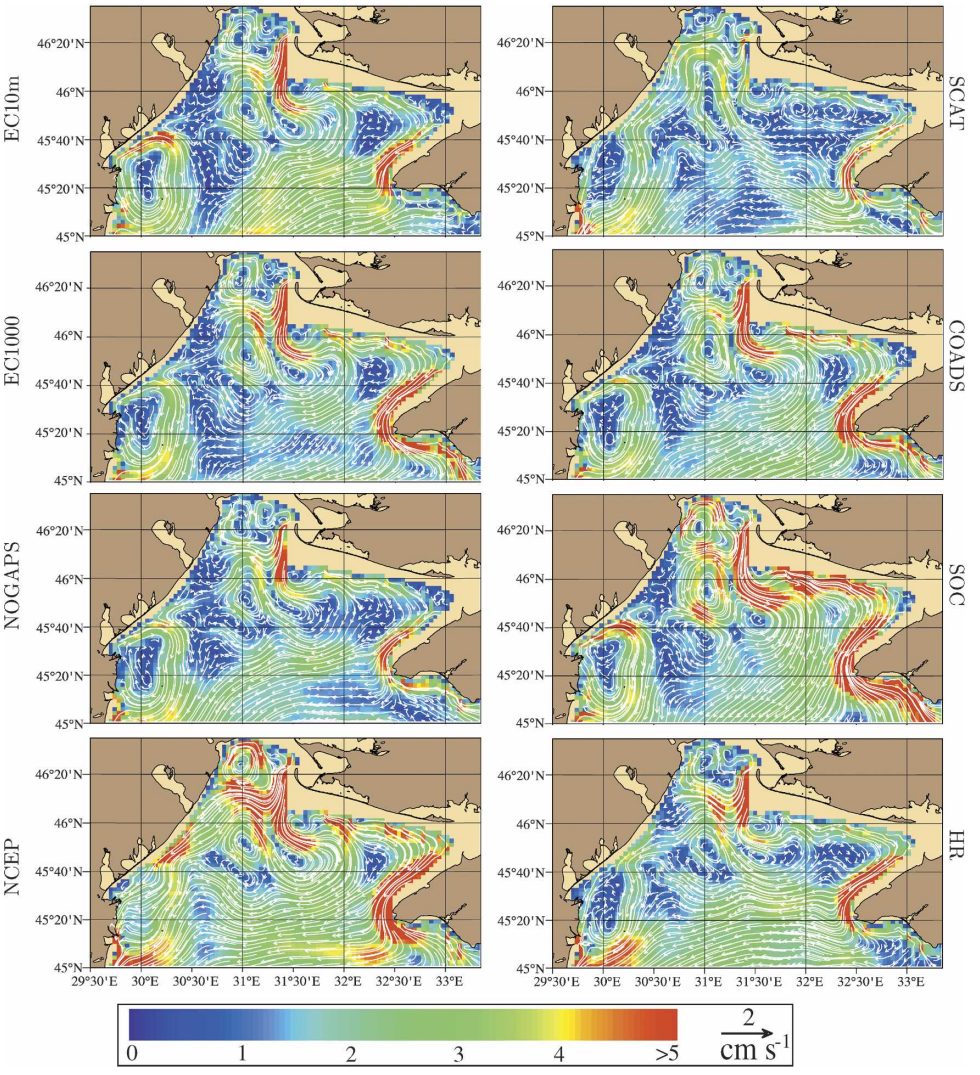

FIG. 13. Same as in Fig. 12, but for currents in a zoom region on a small part of the northwestern shelf where water depths are generally <60 m. Note that the length of the reference velocity vector is 2 cm s^{-1}, and mean current speeds are very weak. The velocity vectors are subsampled for plotting currents obtained from the eddy-resolving (≈3.2 km) HYCOM simulations.